LA-6422

UC-90i

Issued: May 1977

Coal Aerosol Research and Development

1972-1975

Final Report

Charles I. Fairchild
Marvin I. Tillery
Harry J. Ettinger

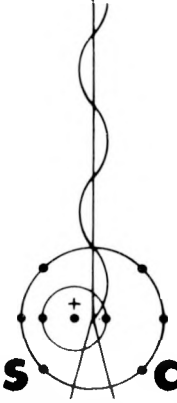

los alamos
scientific laboratory
of the University of California
LOS ALAMOS, NEW MEXICO 87545

UNITED STATES
ENERGY RESEARCH AND DEVELOPMENT ADMINISTRATION
CONTRACT W-7405-ENG. 36

Work supported by the National Institute for Occupational Safety and Health, Project R-072, Cincinnati, Ohio.

Printed in the United States of America. Available from
National Technical Information Service
U.S. Department of Commerce
5285 Port Royal Road
Springfield, VA 22161
Price: Printed Copy $4.00 Microfiche $3.00

CONTENTS

LIST OF FIGURES

LIST OF TABLES

COAL AEROSOL RESEARCH AND DEVELOPMENT

1972—1975

Final Report

by

Charles I. Fairchild, Marvin I. Tillery, and Harry J. Ettinger

ABSTRACT

A program to design and construct hardware systems for testing coal mine air sampling instruments, to develop a reproducible coal test dust, and to investigate the characteristics of one particular personal coal mine sampler has been completed.

Four aerosol test systems were constructed which provided reproducible coal dust aerosols at concentrations up to 6 mg/m^3. These units generated a coal dust environment with a uniformity and stability within ±11% of a desired concentration.

Concurrently, a reproducible log-normally distributed coal dust with size parameters of 3.75 ± 0.25-μm mass median aerodynamic diameter and a geometric standard deviation of 2.1 ± 0.1 was developed. These size parameters were optimum for a single point cyclone calibration, based on the American Conference of Governmental Industrial Hygienists (ACGIH) respirable dust curve.

Calibration of the 10-mm nylon cyclone personal sampler with log-normally distributed coal dusts indicated that a flow rate of 1.7 ℓ/min provided best agreement with the dust separation efficiency specified by the ACGIH curve. Dust loading studies of the same sampler indicated that long-term operation with one type of second-stage filter may result in a significant underestimate of respirable dust. Additional studies conducted in highly electrically charged coal dust clouds confirmed that personal sampler performance is unaffected by this charge.

I. INTRODUCTION

The National Institute of Occupational Safety and Health (NIOSH) has engaged the Los Alamos Scientific Laboratory (LASL), through an interagency agreement, to develop and investigate coal mine air-sampling instruments. Sampling devices used in mines were tested, and equipment to generate a dust accurately simulating a coal mine atmosphere was developed.

A sampling instrument used in U. S. coal mines is the personal respirable dust sampler unit. The sampling head consists of a 10-mm-diam nylon cyclone presampler that separates respirable and nonrespirable dust, followed by a preweighed membrane filter that collects the respirable dust for subsequent gravimetric analysis. The sampler head, attached to the miner's coverall lapel, provides an estimate of the breathing zone respirable dust as opposed to area samplers that estimate the total and/or respirable dust concentration in a general area. The sampling head is connected by flexible tubing to a small belt-carried diaphragm pump powered by a battery pack. This pump contains an in-line pulsation dampener, valve, and flow meter that control and measure the initial flow rate (2 ℓ/min).

To provide assurance that personal sampler units performed satisfactorily, a testing program was needed. LASL undertook to develop and build suitable hardware to provide both the controlled coal dust environment and monitoring instrumentation. The test chamber provided for testing 4 to 12 personal samplers simultaneously along with other samplers.

LASL developed a unique test coal dust to provide an aerosol for 10-mm nylon cyclone testing. This dust had to be reproducible and have well-defined particle size distribution parameters. Typical mine dusts have 2- to 5-μm mass median aerodynamic diameters (MMAD) with geometric standard deviations (σ_g) 2-4.[12] In addition to being similar to mine dust, this test dust was designed to have the optimum size distribution for single point testing personal samplers.

The personal sampler dust separation characteristics have been defined by investigators[3-5,26,27] who used monodisperse aerosols as well as coal dust. However, there is some disagreement about the optimum airflow calibrations. LASL made further calibrations using coal dust aerosols. A number of factors that may affect the cyclone dust separation characteristics were also investigated to determine their importance to field sampling accuracy. These factors include electrical charge on the aerosol and dust loading. Lastly, because the estimate of respirable dust may be affected by second-stage filter collection properties, these collection properties were studied.

II. AEROSOL TEST SYSTEMS

Three aerosol test units with a small aerosol chamber and one unit with a large chamber were built. Although both sizes provided similar capabilities, the differences in construction and operation require separate descriptions. The small units were named Standard Instrument Calibration (SIC) systems; the large unit was called the Standard Coal Aerosol Test System (SCATS).

Both systems were designed to measure the accuracy of personal dust samplers used to estimate workers' exposure to airborne dusts such as coal dust and silica. Each unit can generate a reproducible coal aerosol in which 10-mm nylon cyclone-filter personal samplers can be operated to determine whether the samplers meet performance criteria. This is determined by comparing the measured mass to the respirable mass expected according to the American Conference of Governmental Industrial Hygienists (ACGIH) respirable dust criteria[6] and aerosol size distribution parameters.

The SCATS was designed and built for use at NIOSH in Cincinnati. Although similar to the smaller SIC units in purpose, it had greater capabilities and versatility. The SCATS, with its large aerosol chamber, accommodates more samplers and instrumentation. It also contained a steam injection dryer system for regulation of humidity conditions. Two Wright Dust Feed (WDF) mechanisms were included to permit generation of mixed-component dust clouds.

Three SIC units were built and tested under the interagency agreement. The completed units were delivered to the Engineering Branch, Division of Physical Sciences and Engineering, NIOSH, Cincinnati, Ohio; the Testing and Certification Branch, Appalachian Laboratory for

Occupational Safety and Health, Morgantown, West Virginia; and the LASL Industrial Hygiene Group. NIOSH and LASL each evaluated a prototype unit and suggested improvements for subsequent units.

A. The Standard Instrument Calibration (SIC) System

1. Components. Figure 1 is a front view of the SIC. The system is contained in a cabinet 63 cm (~25 in.) wide, 63 cm (~25 in.) deep, and 155 cm (~60 in.) high. The front panel contains controls and monitoring instruments for the system. Periodic monitoring of the aerosol mass concentration is provided for by the GCA Corporation Respirable Dust Monitor (RDM). Control and monitoring of airflow to the aerosol generator (WDF) and dilution air for the aerosol chamber are provided by the airflow control panel. This panel also provides six suction lines with on-off snap valves, needle valves for flow rate control and rotameters for flow rate monitoring for the sampling instruments to be calibrated. Rotameters also indicate the flow rate of aerosol generator and dilution air. The electrostatic precipitator control panel provides for control and monitoring of high voltage for a precipitator that collects samples for electron microscopy (EM). A magnehelic gauge with a range of ±0.5 in. of water indicates pressure differential between the aerosol chamber and atmosphere.

Figure 2 is a rear view of the SIC system showing the aerosol chamber, WDF aerosol generator, tritium deionizer, mixer-diluter, point-to-plane electrostatic precipitator, and sampling pump. A detailed description of the important components follows.

a. Aerosol Chamber. The aerosol chamber has a volume of 25 ℓ. The chamber, constructed from polyethylene, is a right circular cylinder of 25-cm diam with a conical bottom and an overall height of 46 cm. Four peripheral sampling ports are located around the side of the chamber as shown in Fig. 3. Aerosol from the generating system enters the conical bottom through a mixer (Fig. 4). Clean air also enters the mixer through several converging nozzles to dilute the aerosol to the desired concentration. A 1-cm-thick transparent plexiglass plate seals the top of the chamber and permits viewing the interior during operation. Five holes in this plate serve as passthroughs for four personal samplers and an exhaust tube. Aerosol is exhausted through a baffled 2.5-cm-diam Tygon tube to four high-efficiency, particulate respirator filters connected in parallel. Four peripheral sampling ports, plus four of the top ports, permit withdrawal of aerosol samples or insertion of sampling probes into the test chamber through rubber stopper seals.

A bypass outlet on each side port of the chamber (Fig. 3) permits isokinetic sampling at each port even though the sampling devices may require different flows. The total flow from each port can also be the same, even though the sampling instruments withdraw aerosol at different rates. This capability permits symmetrical sampling from the relatively small chamber.

b. Wright Dust Feed Mechanism.[7] This device (Fig. 2) disperses dust into the airstream at a predetermined, uniform rate. A cylindrical cup containing compacted dust, is inverted and threaded firmly to a base. The cup, while rotating, slowly descends against a stationary scraper blade that continuously removes dust from the compact surface. Compressed air entering the cup through an orifice sweeps across the scraper blade and entrains and removes particles at a uniform rate. Both the airflow and cup rotation rates can be varied to provide a wide range of aerosol concentrations.

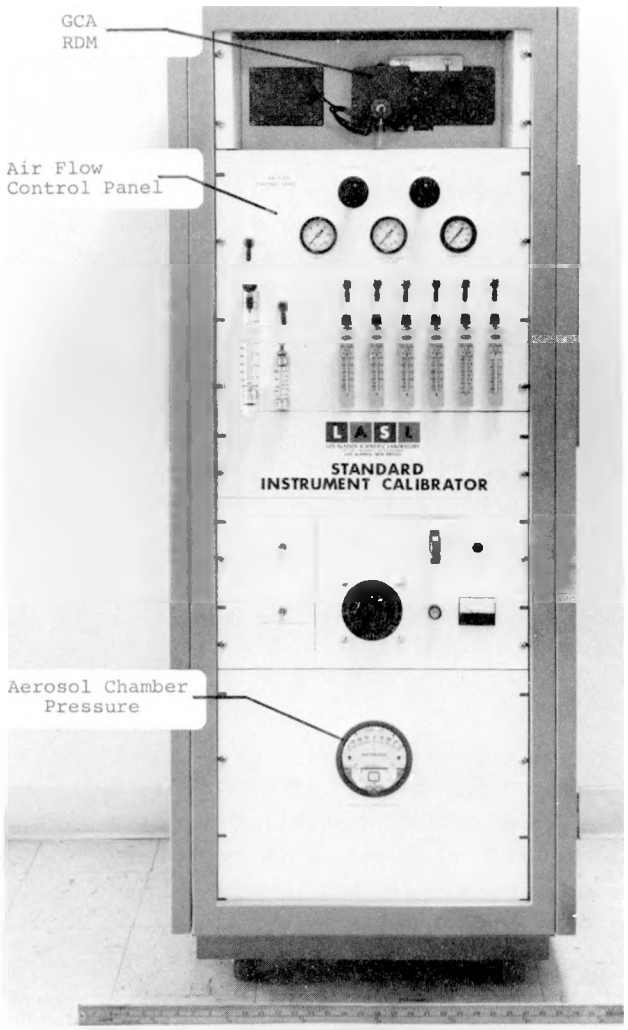

Fig. 1.
Standard Instrument Calibration System (SIC) (front).

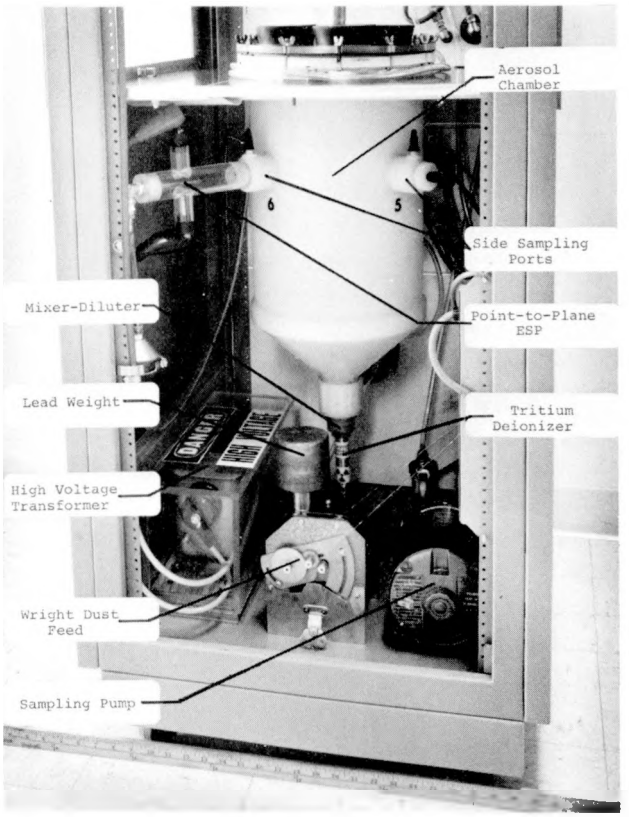

Fig. 2.
SIC lower section (rear).

c. Aerosol Charge Neutralizer. As dust particles are generated in the WDF and introduced into the airstream, they acquire electrical charge that affects their behavior and the dust cloud properties. Before the aerosol is introduced into the experimental chamber, the cloud's overall electric charge is neutralized by passing the aerosol stream through an intense ion concentration created by β^- emission from tritium. A stainless steel foil lining a cylindrical case has 200 mCi of tritium as titanium tritide plated on its inner surface. The chemical stability of titanium tritide minimizes radioactive contamination. Periodic washing of the foil to remove deposited particles results in less than 0.02 μCi/ml of tritium in the wash water which constitutes no health problem. The brass case (Fig. 5) encloses the tritide foil, distributes aerosol flow through an annulus and past the foil, and prevents personnel contact with or exposure to the tritium.

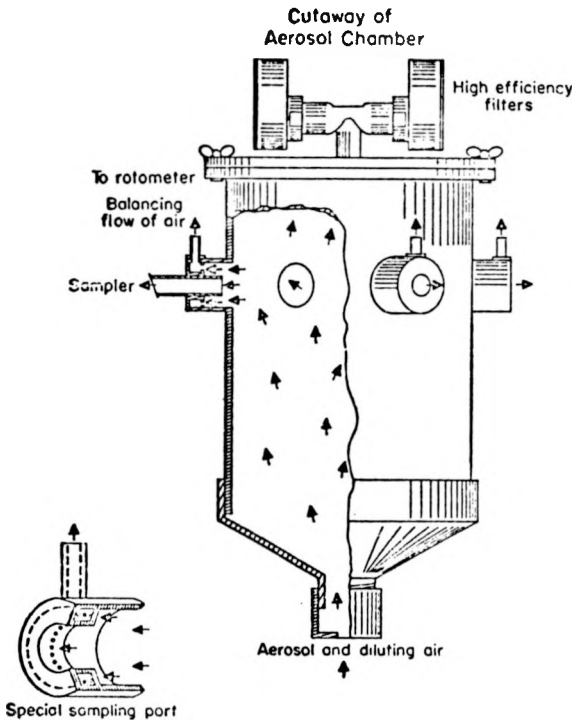

Fig. 3.
Cutaway of aerosol chamber and special sampling port.

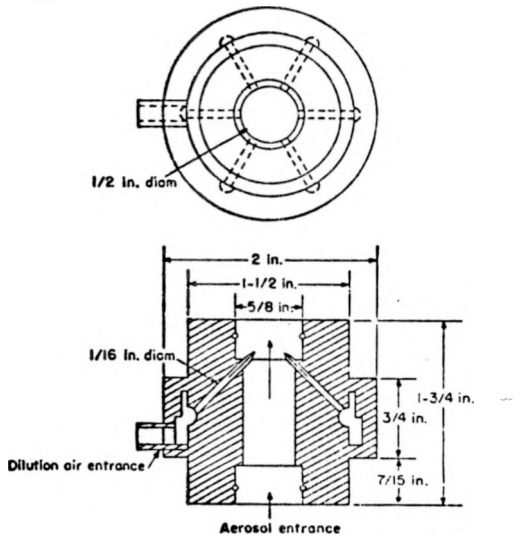

Fig. 4.
Aerosol dilution-mixer device.

d. GCA Respirable Dust Monitor.[8] This sampler (Fig. 1), designed specifically to sample coal dust, provides a means for continuously monitoring aerosol mass concentration during 1-min sampling intervals at a 2-ℓ/min flow rate. The instrument consists of an impactor, β^- counter, power supply, sampling pump, and electronics. It collects coal dust particles >0.7 μm in diameter by impaction on a petroleum-jelly coated Mylar collection foil positioned between 100 μCi of ^{14}C and a counter. Attenuation of the β^- radiation by deposited coal dust is measured and displayed as mass concentration. If a cyclone presampler is placed in the flow stream ahead of the RDM, the respirable dust passing the cyclone can be measured. The RDM model installed in the SIC system can measure 1.0- to 50-mg/m³ coal dust concentrations with ±25% accuracy at the 95% confidence level. Although the unit is self-contained and portable, it is used as a stationary instrument in the SIC system.

e. Electrostatic Precipitator. A single stage, point-to-plane electrostatic precipitator (Fig. 2) similar to a glass envelope precipitator previously used at LASL,[9] is used to collect particles on electron microscope grids for subsequent analysis. A 3-mm-diam grid is mounted on the planar electrode approximately 3 cm from a vertical needle electrode. A plexiglass precipitator housing directs the aerosol flow (4 ℓ/min) between the electrodes. A high-voltage power supply provides a 9-kV ac potential across the electrodes. Because this power supply can produce a 10-kV, 5-mA discharge, the circuit contains a limiting resistor to control available amperage.

2. System Operation. Proper SIC system performance requires careful preparation and operation. A step in the preparation procedure is formation of the WDF powder compact. This device's output largely determines concentration stability with respect to time, and poor pressing technique will cause fluctuations in aerosol concentration. Excessively porous or nonuniform compacts may be rapidly eroded by the airstream, or, if the compact surface is very hard, the scraper blade may not cut uniformly. The optimum compacting load depends upon size distribution, moisture content, and composition of the bulk dust. Pressures of 350 to 700 kg/cm^2 have proved satisfactory for the bulk coals used at LASL. Dust compacts pressed at these pressures form weak but coherent bodies. Dust scraped from the compact and particles that adhere together are separated by the turbulent, high-shear air forces at the exit of the WDF. The shearing action in the WDF generates triboelectric charge on the particles that is neutralized by the tritium β^- source before the aerosol enters the test chamber.

The prototype test unit used a 4-Ci tritium aerosol charge neutralizer. The minimum activity required to neutralize particles at the expected concentration and flow rate was determined both theoretically and experimentally as described in the Appendix. Calculations indicated that 228-mCi activity was required; however, experiments indicated that 125 mCi of activity was sufficient to neutralize the charge on an actual coal dust aerosol. Thereafter, the charge neutralizers were limited to 200 mCi of tritium.

Chamber and WDF airflow is controlled by pressure regulators, and flow meters on the front panel (Fig. 1) of each unit. Compressed air at 30-50 psig enters through an air filter and is reduced in pressure and distributed to flow meters (Fig. 6) at 20 psig. Airflow to the WDF is normally 30 ℓ/min, and the normal dilution airflow is 90 ℓ/min. Depending upon required dust concentration and flow velocity either flow can be varied. Air flowing through the WDF drops from 14 psig at the inlet to slightly above ambient pressure at the exit. The aerosol then passes through the neutralizer and the dilution mixer before entering the chamber at essentially atmospheric pressure.

As aerosol enters the chamber it is deflected by a mixing baffle to prevent formation of a center jet. Aerosol flows of 60 to 120 ℓ/min produce average air velocities of 3.5 to 5.0 cm/s in the cylindrical section of the chamber, resulting in at least two air changes per minute.. The chamber's low flow velocity permits sampling from an essentially static environment without concern for isokinetic sampling. Either straight or 90° probes may be used to conduct aerosols from each of the side ports through "in-line", 25-mm-diam filter holders connected directly to the probes at the chamber port. Polyvinyl chloride (PVC), 0.8-μm pore size, membrane filters were generally used to collect samples at 2 ℓ/min for 12 to 15 min.

Although dust concentration in the chamber can be determined gravimetrically within 20 min via membrane filters, it is desirable to monitor the concentration by a faster, less tedious method. Two commercial fast-response instruments were evaluated for this purpose.

One unit, manufactured by Thermo-Systems, Inc. (TSI) is the particle mass monitor (PMM). This instrument operates by electrostatically precipitating the aerosol particles onto a vibrating quartz crystal and periodically measuring the change in vibrational frequency caused by the deposit.[10] This change is referenced to the vibration frequency of a similar noncollecting crystal, and the frequency difference between the two is printed at regular intervals. Mass concentration can be calculated from known constants and the frequency change. The quartz crystal PMM proved marginally useful in the SIC system owing to crystal overload resulting in low dust concentration measurements compared to membrane filter samples. Crystal overload occurs because the outer layers of a dry coal dust deposit do not adhere as well as the initial deposit and thus do not have the same effect on vibration frequency. The onset of this phenomenon depends

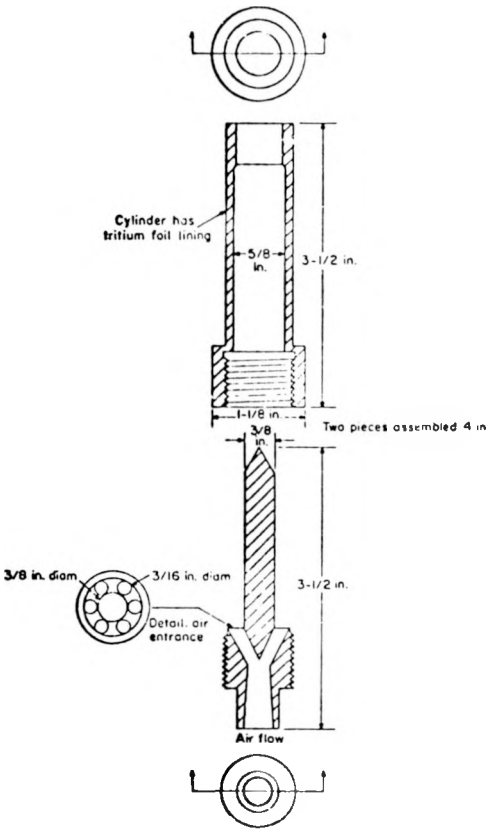

Fig. 5.
Aerosol charge neutralizer detail.

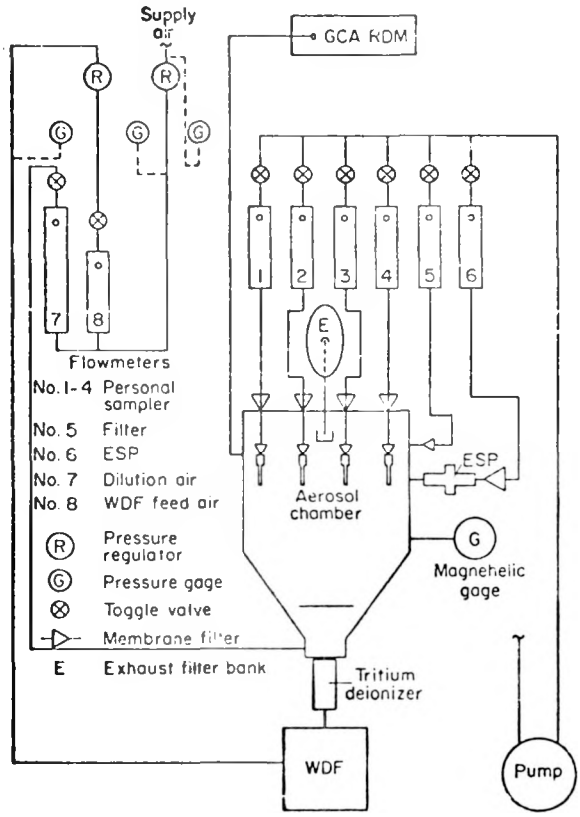

Fig. 6.
Airflow schematic.

upon the particulate material, but in coal dust it occurs in <2 min at 4-$\mu g/\ell$ concentration. Therefore, the crystal collection surface required frequent cleaning. Consistent low concentrations, 25% below those shown by filter samples, (Fig. 7) appeared to be due also to losses in the sampling system. Shortening the sampling tube from 46 cm to 10 cm decreased the line loss slightly, resulting in PMM results approximately 15% lower than gravimetric results. Tests of the PMM precipitator collection efficiency showed that nearly all particles were deposited; consequently, low particle concentration seems to be a function of both transport line loss and poor interparticle cohesion in the deposit.

A GCA Corporation RDM[8] was evaluated as the second fast response mass concentration indicator. The RDM has some drawbacks, but it is simpler to operate and can function at higher mass concentrations. Initial RDM calibration agreed with a GCA-supplied standard sample, but the indicated dust concentration was higher than that shown by simultaneous gravimetric measurements made with membrane filters (Fig. 8). RDM measurements were adjusted to correspond to the mass indicated by these filters (Fig. 9) by correcting the instrument calibration. In addition, calibration drifted such that adjustment was necessary after approximately 100 readings. By controlling oscillator frequency using a frequency counter, it was possible to adjust the RDM readout to correspond to membrane filter measurements. Even so, individual instrument readings varied, giving an average coefficient of variation of 27%. However, these

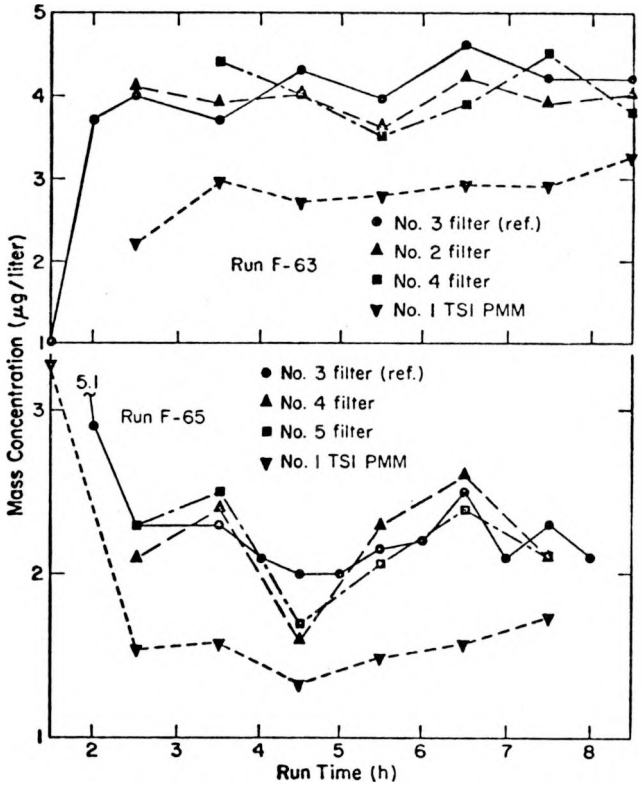

Fig. 7.
Mass concentration data plot.

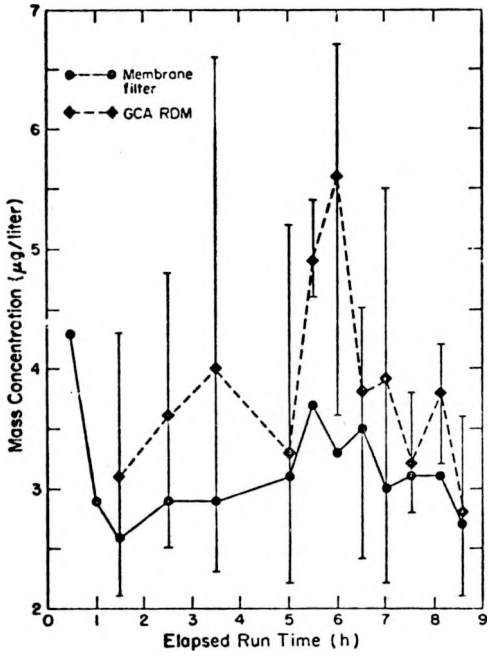

Fig. 8.
Mass concentration in SIC chamber, dispersion run F-78.

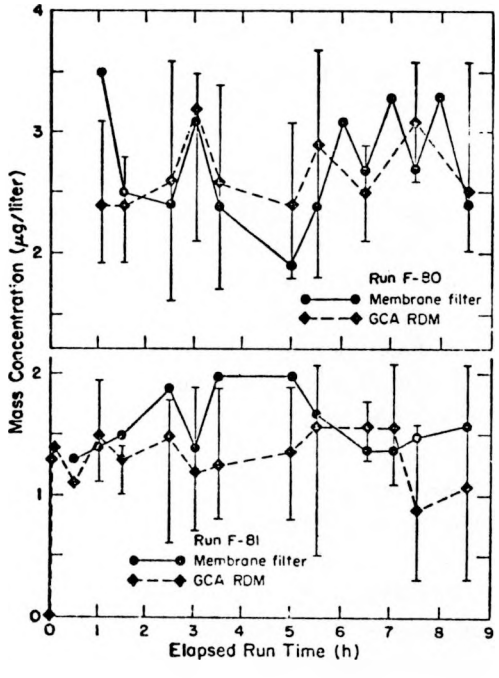

Fig. 9.
Mass concentration in SIC chamber, dispersion runs F-80 and F-81.

variations may be valid because filters average out concentration fluctuations over a 15-min sampling period compared to the RDM's 1-min cycle time. The RDM also showed some sampling line loss, so it performed best when placed very near the aerosol source.

3. Performance. The three SIC aerosol test systems performed similarly. Slight differences were generally due to different test conditions such as concentration level and number of samplers used. Samples for aerodynamic and microscopic particle size determination, personal sampler comparison, and mass determination often were collected simultaneously. Withdrawal of more than 10% of the total aerosol flow at one sampling port, as was done with the Andersen impactor (AI), disrupted the cloud uniformity for as long as 30 min after sampling ceased.

Starting the units with a new dust plug produced an unstable concentration, lasting up to 2 h, (e.g., Figs. 7 and 8). Restarting with the same plug caused milder variations which persisted <30 min. Because of these startup instabilities, no sampling other than mass monitoring was performed during the initial 2 h of operation. After that, the units provided aerosol stability of ±11% (coefficient variation) or better. Stability is defined as the variation of mass concentration with time at a single location. Uniformity is defined as the time-independent variation of concentration measured simultaneously by three or more samplers at spaced locations. Uniformity of mass concentration at different sampling locations within the units was likewise ±11% or better. These parameters were measured during experiments in which no other samples were withdrawn and the chamber was not disturbed. Mean concentration values obtained in individual dispersion experiments from filter, TSI PMM, and GCA RDM measurements are listed in Table I. Filters 1-3 represent samples taken simultaneously at positions 15 cm apart within the chamber. Each value, except those for the RDM, is the average of five or more samples. Each RDM concentration is the average of six samples, so each concentration for this instrument represents a minimum of 30 readings. Mass concentration stability and uniformity are shown in the last two columns. As discussed, values determined using the PMM and RDM average 25.4 and 6.5%, respectively, lower than membrane filter determinations.

Physical size distribution of the dust cloud was measured by standard electron microscope techniques applied to samples collected by the point-to-plane ESP. As well as providing sizing information, electron miscroscopy in conjunction with optical microscopy of membrane filters showed that the aerosol did not agglomerate.

To estimate aerodynamic particle size characteristics, an AI operated at 28.3 ℓ/min was used to fractionate the dust according to aerodynamic diameter. The impaction plates were covered with preweighed 81-mm-diam PVC membrane filters to provide low tare weight collection surfaces and minimize particle rebound. Generally, two or three AI samples were taken during each dispersion experiment; sufficient mass was collected in 20-min sampling periods to permit size analysis by weight. A Mettler microbalance with ±5-μg precision and a 200-μg sample size provided ±5% accuracy. The data were used to compute and plot a cumulative size distribution on log-probability graphs. Almost all the dusts were log-normally distributed. Generation of aerosols from the same bulk dust gave a run-to-run size distribution reproducibility of ±6.5% in MMAD. This is the average of the coefficients of variation for all AI data.

Relative particle size distribution stability within the chamber was measured using 10-mm nylon cyclones. Three cyclones were suspended in the chamber about 10 cm apart, and operated at 1.7 ℓ/min for 3/4-4 h. Respirable dust that passed the cyclone was collected by 47-mm-diam Gelman, type VM-4, membrane filters which have high flow resistance but a very low stable tare weight. This low tare weight, combined with ±5-μg balance precision produced better than ±2%

TABLE I

AEROSOL TEST SYSTEM MASS CONCENTRATION PARAMETERS

Run	Average Mass Concentration (μg/ℓ) Filters 1	2	3	TSI PMM	GCA RDM	Stability (%)[a]	Uniformity (%)[b]
Unit 1							
F-63[c]	4.1	4.0	4.0	2.8		6.3	6.7
64[c]	2.9	2.8	3.0	2.5		10.2	8.3
65[c]	2.2	2.2	2.2	1.6		12.0	6.1
67[c]	2.1	2.2		1.9		17.2	
Unit 2							
F-77	2.0	2.3	2.0			16.1	13.5
78	3.1	3.4	3.2	2.1	3.9	15.9	13.8
79[c]	3.8	3.5	3.8	2.2	2.3	10.1	3.9
80	2.6	2.8	2.6	1.9	2.7	23.6	24.0
81	1.6	1.6		1.8	1.4	18.0	
82	3.4	3.1		1.8	3.1	20.2	
Unit 3							
84[c]	2.5	2.7	2.3	1.5		11.2	11.6
87	2.7	2.8		2.2	2.6	18.2	
88	3.4	3.3			2.1	8.2	
89	4.1	4.0			3.7	10.4	
90	2.3	2.4			2.5	17.2	
92	1.7	1.7	1.7			18.9	12.1
93	1.5	1.6	1.6			15.3	10.8
94	0.8	0.9	0.9			40.4	21.1
95	3.3	3.5	3.4			11.0	6.9
96	2.9	3.0	2.8			11.0	9.0
97	3.3	3.3	3.4			12.8	9.5
98	3.1	3.4	3.4			17.8	8.7
99	3.5	3.4	3.4		3.6	13.0	6.4
101	4.1	4.0	4.0		3.3	8.9	4.6
102	4.0	4.3	4.1		3.1	8.1	7.1
103	3.9	4.0			2.7	3.3	
104	4.7	4.7			3.0	5.8	

[a] Variation of mass concentration at one location with respect to time.

[b] Variation of mass concentration measured simultaneously at three or more locations. Variation was measured each hour during run.

[c] Test runs with constant aerosol flow, no chamber disturbances, and 2½-h cloud stabilization time before measurements started.

mass sensitivity. Agreement among cyclones, defined by an average coefficient of variation (mean variation), was ±12%. The AI sizing results and 10-mm cyclone filter penetration results are shown in Table II.

B. The SCAT System

The major difference between SCATS and its predecessors is the size of the aerosol chamber (Figs. 10 and 11), a 46-cm-diam by 183-cm-high cylinder. This chamber can simultaneously accommodate six or more personal samplers, a British Mining Research Establishment horizontal elutriator, and probes for other aerodynamic sampling instruments. This design provides 47-ℓ/s (100-cfm) airflow capacity at 6-mg/m³ dust concentration and 25-cm/s flow velocity in the sampling region, with a flat velocity profile across 80% of the chamber diameter. In addition to a top mounted centrifugal fan, and high-efficiency filters at each end, the unit incorporates two

TABLE II

AERODYNAMIC SIZE PARAMETERS AND CYCLONE PERFORMANCE

		Andersen Impactor			10-mm-Diam Nylon Cyclone			
Run	Dust	MMAD (μm)	Coeff Var	σ_g	Penetration (%)	Std Dev	Coeff Var	No. of Samplers
95	Na-1:18	4.0 ± 0.1		1.8 ± .1				
96	Na-1:18	3.7 ± .1		2.1 ± .1				
98	Na-1:18	4.5 ± .1		2.1 ± .1				
Av	Na-1:18	4.0 ± .4	0.10	2.0 ± .2				
99	B-23-31	3.5 ± .1		1.9 ± .1				
100	B-23-31	3.6 ± .1		1.9 ± .1				
Av	B-23-31	3.6 ± .1	0.04	1.9 ± .1				
101	B-21-24	3.7 ± .1		2.0 ± .1				
102	B-21-24	3.6 ± .1		1.9 ± .1				
103	B-21-24	3.6 ± .1		1.9 ± .1	42.7	4.0	0.09	6
Av	B-21-24	3.6 ± .1	0.03	1.9 ± .1				
104	B-3-1	4.3 ± .2		1.9 ± 0	35.6	3.3	0.09	6
105	B-3-1	4.2 ± .3		2.0 ± .5	37.2	7.4	0.20	6
106	B-3-1	4.0 ± .6		2.0 ± .1	36.2	5.2	0.14	6
107	B-3-1	4.0 ± .4		1.9 ± .1	34.9	4.6	0.13	4
108	B-3-1	4.0 ± .1		2.1 ± .1	31.9	3.9	0.12	5
Av	B-3-1	4.1 ± .3	0.07	2.0 ± .1	35.2	4.9	0.14	
109	B-5-1	3.8 ± 0		2.2 ± 0				
110	B-5-1	4.0 ± .3		2.1 ± .1				
111	B-5-1	3.8 ± .3		2.2 ± 0				
112	B-5-1	3.7 ± .2		2.0 ± .1	42.0	8.7	0.21	7
113	B-5-1	3.7 ± .2		2.1 ± .1	37.5	2.5	0.07	6
114	B-5-1	3.6 ± .3		2.1 ± .1	47.7	3.3	0.07	10
Av		3.8 ± .2	0.06	2.1 ± .1	42.4	4.8	0.11	
116	SC-3	3.8 ± .3	0.09	2.2 ± .2	46.2	3.1	0.07	6
Mean Variation			0.06				0.12	

WDFs, two 200-mCi tritide charge neutralizers, a RDM, a humidity control unit, and a temperature and relative humidity indicator. The humidity control unit enables chamber operation over a range from 10 to 90% relative humidity. Dehumidification was provided by a commercial, regenerative, adsorption-type dehumidifier, and a humid environment could be provided by steam injection through a distributor pipe. The SCATS can be operated in a single-pass or recycling mode. The use of two WDFs permits generation of two different particulate materials over a wide range of proportions. As described below, the SCATS performance meets the specifications of 4.7×10^{-3} m^3/s (100-cfm) aerosol flow, a flat velocity profile (±15%) over 80% of the diameter at the sampling level, and a uniform mass concentration in this same region.

During operation with recycled, dehumidified air the chamber temperature may be 10 to 12°C above ambient because of heat transfer to the air by exothermic moisture adsorption and high-temperature regeneration cycles in the dehumidifier. Velocity profiles were determined by measurements at nine locations at each sampling level. At least two velocity readings were taken at each location. As only one probe was available, these measurements were not simultaneous: one complete set of measurements was made before a second set was started.

Performance characteristics measured for single-pass and recycled flow configurations are presented in Table III. The initial measurements (Runs 1-6) indicate that the pressure drop through a paper prefilter, already high, increased rapidly when dust was introduced into the

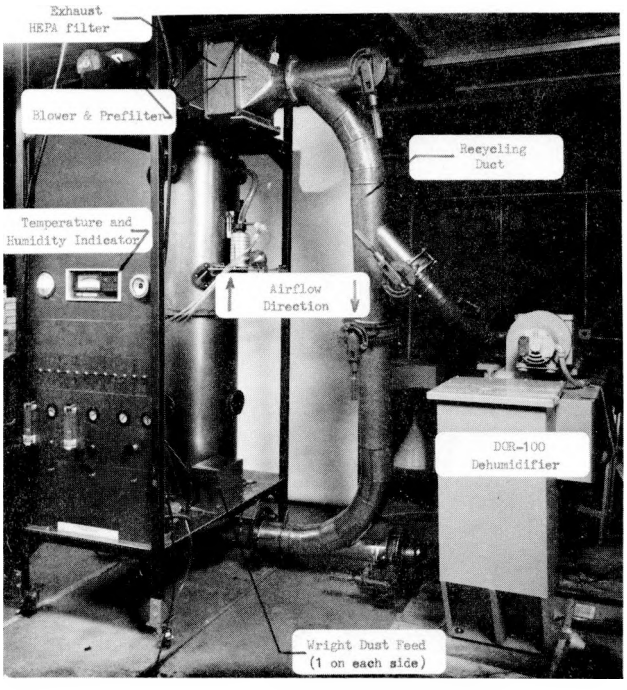

Fig. 10.
Standard Coal Aerosol Test System (SCATS).

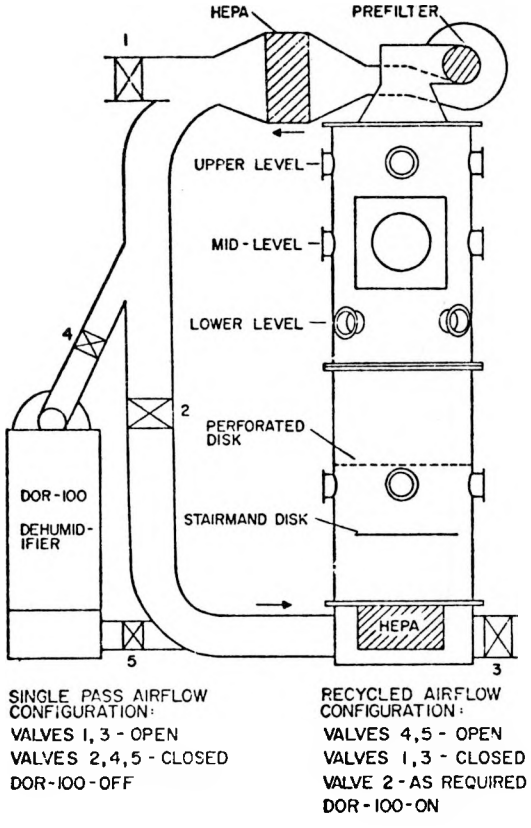

Fig. 11.
SCATS airflow control and valving configuration.

TABLE III

SCATS PERFORMANCE CHARACTERISTICS

Test Configuration[a]	RH (%)	T (°C)	Flow Velocity[b] (cm/s)	Mass Conc[c] (mg/m³)
1. S.P., L.L.[d]	10	23.3	14.8 ± 1.9 (13)[e]	2.6 ± .2 (8)[e]
2. S.P., M.L.[d]	7	29.4	13.9 ± 1.5 (11)	2.3 ± .4 (18)
3. S.P., U.L.[d]	7	32.8	13.8 ± 1.0 (7)	2.5 ± .2 (8)
4. M.P., L.L.[d]	5	33.9	20.4 ± 5.6 (27)	2.3 ± .2 (10)
5. M.P., M.L.[d]	6	32.2	19.7 ± 3.9 (20)	2.5 ± .2 (6)
6. M.P., U.L.[d]	5	35.6	19.3 ± 2.5 (13)	2.6 ± .2 (8)
7. S.P., L.L., F.C.	8	21.1	23.7 ± 2.8 (12)	1.5 ± .1 (8)
8. S.P., M.L., F.C.	8	23.9	24.3 ± 1.4 (6)	1.6 ± .1 (6)
9. M.P., M.L., F.C.	5	35.6	28.3 ± 2.1 (7)	1.6 ± .1 (8)
10. M.P., M.L., F.C.	5	35.6	27.4 ± 1.3 (5)	1.7 ± .1 (7)

---

[a]Test configuration: S.P. - single-pass airflow
M.P. - multipass airflow with recycle flow passing through dehumidifier.
L.L. - lower level sampling port cross section.
M.L. - midlevel sampling port cross section, level with large access port.
U.L. - upper level sampling port cross section.
F.C. - final chamber configuration.

[b]Mean of at least 18 readings.

[c]Mean of at least five samples.

[d]Measurements made before installation of perforated disk and transparent fairing. These changes were included in the SCATS unit shipped to NIOSH, and the improved performance characteristics are indicated by the remaining tests.

[e]Numbers in parentheses are coefficients of variation.

chamber. This prefilter was replaced with a 1-cm-thick, cylindrical, fibrous cotton filter that reduced the pressure drop. Airflow through the cotton prefilter was from the outer to the inner cylindrical surface. This prefilter permitted 8-h dust loading without appreciable changes in pressure and flow velocities. Also, velocity profile measurements revealed significant flow distortion at the large access port. A transparent fairing was placed inside this opening to smooth the chamber contour. A perforated disk was installed in the lower chamber, 23 cm above a Stairmand disk, to further improve the velocity profile.

Data in rows 7-10 of Table III were obtained after the cotton prefilter was installed and the chamber was modified. These changes improved the velocity uniformity, particularly at the midlevel sampling positions. The air velocity in the final, single-pass flow configuration is slightly less than the sea level design velocity, because the air density is approximately 20% less at Los Alamos than at sea level. Air velocity is greater when the dehumidifier is in use due to the additional blower.

All mass concentrations in the final column of Table III were determined after the cotton prefilter was installed, but only the final four runs were made after installation of the access port fairing and perforated disk. Concentrations were measured simultaneously at five uniformly spaced sampling points at each sampling level, using membrane filters and a 15- to 20-min sampling period with all sampling probes facing downward into the airstream. One sample, taken at the center of the chamber 1 h before the sampling started, showed the same concentration and indicated that the concentration is stable.

Replicate (four separate determinations) size distribution measurements made with a six-stage AI operating at 28.3 ℓ/min during the SCATS performance tests indicated that the dust size parameters were 3.8 ± 0.2 μm and a σ_g of 2.3 ± 0.2. These compare to previous measurements of 3.7 ± 0.2 μm and 2.2 ± 0.2 for the same dust made in the smaller SIC unit.

C. Conclusion

The aerosol in all units is generated by a WDF mechanism at a uniform rate, with few particulate agglomerates, and a stable size distribution. After passing through an electric charge neutralizer and a mixer and diluter, the aerosol enters a chamber where its velocity is reduced to produce laminar flow. Mass concentration variation is less than ±10% from point to point within the chamber. Control of concentration is critical because any nonuniformity would indicate a false variation in sampler collection efficiency. Aerosol mass concentration measurement is determined primarily by accurate gravimetric measurement of samples collected on membrane filters. Immediate indication of concentration is also obtained from a fast response sampling instrument.

Other important parameters in personal sampler tests are the aerosol aerodynamic particle size distribution and that distribution's stability throughout a test. Particle size distribution is primarily controlled by the bulk dust particle size distribution. It is also affected by generation conditions, airflow fluctuations, particulate charge, and velocity and time in the chamber. Aerodynamic sizing of samples from the SIC System indicates that the variation in size distribution is less than ±6%.

The SIC units have been used satisfactorily to test personal samplers. They have also been used to investigate charge effects on 10-mm-diam nylon cyclones,[11] and to determine operational characteristics of personal sampler pumps.[12] The SCATS has been used to determine charge effects in dispersion of PVC dust.[13]

III. STANDARD COAL DUST

NIOSH initiated the development of a standard test coal dust in 1971 when they became responsible for testing and certifying coal mine air-sampling instruments, such as the 10-mm nylon size-selective personal samplers. These samplers provide a good estimate of a worker's exposure only if their collection characteristics meet criteria for respirable coal dust sampling. Therefore, some fraction of the samplers destined for field use should be checked to confirm calibrations made previously using laboratory test aerosols and to provide quality assurance for production models. To provide a realistic environment for these tests (and for reasons discussed in the next section), coal dust was selected as the challenge aerosol. It was also considered necessary that the test aerosol particle size characteristics approximate those of dust clouds encountered in mines.

A. Properties of a Standard Dust

A standard dust must be reproducible, easily dispersed, of low toxicity, and susceptible to accurate mass measurement. Less important are unit density, chemical purity, known aerodynamic particle shape factors (e. g., spherical particles), availability, and low cost. Unfortunately, no available material meets all these criteria. Of the readily available, easily handled dusts, coal is useful because it is the material of concern and substitutes offer no advantage if coal dust can be produced, characterized, and used accurately and economically. Its composition and density vary from mine to mine, but dust can be produced from one large homogeneous batch of coal. A Pennsylvania bituminous coal from one area of a designated mine was used.

B. Theoretical Considerations

A standard dust used to test respirable dust air-sampling instruments must contain a large percentage of particles in the respirable size range. A dust cloud generated from the standard is then separated by the instrument into respirable and nonrespirable mass fractions according to aerodynamic size.

Theoretical calculations by Moss[14] and Lynch[15] provide some insight into the selection of possible polydisperse dusts for calibrating the responses of various instruments. These calculations show that as the geometric standard deviation of a fixed median diameter, log-normal, aerosol distribution increases, the respirable mass fraction changes. However, all such distributions with a MMAD of 3.75 μm will have 46% respirable mass regardless of the dispersity (σ_g) of the dust (Fig. 12). Thus a theoretical common collection efficiency exists for a log-normally distributed aerosol with a 3.75-μm MMAD. These data are replotted with the same ordinate in Fig. 13 but with σ_g as the abscissa, again showing that 46% of the mass of a 3.75-μm MMAD aerosol is respirable regardless of σ_g.

The effect of MMAD deviations from 3.75 μm on the respirable fraction of a real aerosol can be evaluated. Some uncertainty in controlling or measuring the MMAD is normal. If the coefficient of variation (standard deviation/mean of samples) for the sizing method is $\pm$6%, an aerosol with a measured MMAD of 3.75 μm has a 72% probability of having a true MMAD between 3.5 and 4.0 μm. A monodisperse aerosol in this size range has 41 to 52% respirable mass (Fig. 12). A polydisperse aerosol with the same uncertainty in MMAD but with σ_g = 2.0, would be 43-50% respirable. Thus, as the dispersity (σ_g) increases, a given MMAD deviation produces a smaller variation in penetration. In other words the penetration curves become more nearly horizontal and closer to the 3.75-μm MMAD curve as σ_g increases. This is further clarified in Fig. 13, a replotting of Fig. 12, with σ_g as abscissa and parametric curves of constant MMAD. At 3.75-μm

MMAD, theoretical penetration is constant at 46%. Figure 13 also shows that the uncertainty in respirable dust fraction is smaller at large σ_g for a given deviation or uncertainty in MMAD about 3.75 μm.

Dust agglomeration may affect performance of size selective air-sampling instruments, due to changes in apparent density and aerodynamic shape factor, thus particle agglomeration in a test dust must be insignificant.

Based on these considerations, specifications for the standard test dust were as follows.

1. A Pennsylvania bituminous coal shall be used as specified by NIOSH to provide a standard bulk material.
2. The airborne dust size distribution shall be approximately log-normal.
3. The airborne size distribution parameters shall be 3.75 ± 0.25-μm MMAD and $\sigma_g \geq 2.0$ with a standard deviation of ±0.1.
4. The airborne dust shall show no significant particle agglomeration at 4-mg/m^3 mass concentration.

C. Experimental

Coal for development of the standard dust was received in chunks. It was passed through a jaw crusher to reduce the maximum particle size to approximately 4 mm, mixed thoroughly, and separated into eight 5-kg portions. These portions provided a convenient volume for further processing.

1. Comminution. Two methods for further reducing the coal to a usable size distribution were evaluated. Ball milling and fluid energy milling were selected because both produce small particles, although each has disadvantages. Ball milling is a batch process that may require a

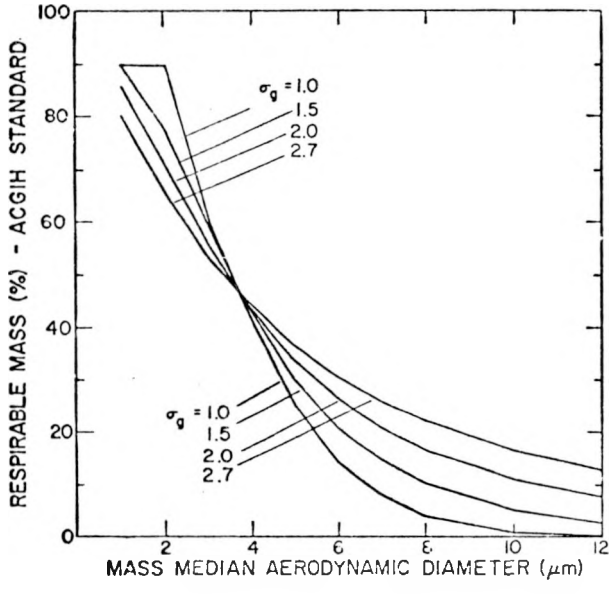

Fig. 12.
ACGIH dust penetration efficiencies for log-normally distributed polydisperse dusts.

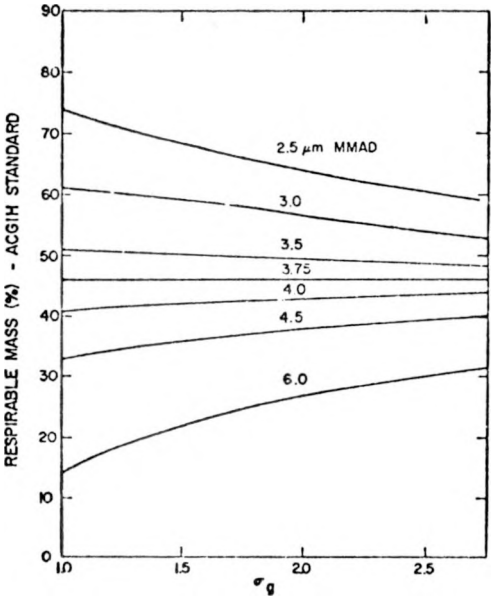

Fig. 13.
ACGIH dust penetration efficiency as a function of σ_g.

long time to produce a small particle size, and the product size distribution is quite disperse. On the other hand, fluid energy milling and centrifugal selection can waste much of the starting material, yet provide a fairly narrow size fraction. The degree of milling was determined by the change in measured specific surface.

Ball milling was performed in a 1-ℓ ceramic mill containing a 200-g charge of coal plus 500 g of assorted 1/8- to 3/4-in.-diam stainless steel balls. The jar contents were milled at 30 rpm for up to 8 h. Due to the softness of the bituminous coal, 97% of the size reduction occurred in the initial 1 h of grinding (Fig. 14). The effect of milling is shown by the increased specific surface. The product was approximately the same after 4 h because some large balls (3/4-in. diam) were not used during this period. Although the milling was efficient, the product agglomerated and was difficult to disperse.

Simultaneously, experiments were conducted to determine the feasibility of fluid energy milling. A small laboratory Micronizer mill was used to grind -35/+100 mesh coal. This mill grinds particles against one another at high impact velocity within a conical chamber. The coal is fed into a conical hopper and entrained by an air ejector for transport to the grinding chamber. Another high-pressure airstream enters the grinding chamber from several tangential inlets to produce intense turbulence and particle collisions. Centrifugal forces from the spiral circulation keep oversize particles from leaving the conical chamber. Below the grinding chamber, a separation chamber (cyclone) containing a vertical exhaust pipe removes fine particles with the air; the product particles are deposited in a container below the separation chamber.

Comminution experiments utilizing this fluid energy mill established that the product particle size depends largely on air pressure, and to a lesser degree upon grinding time. Air pressure <35 psig produced little grinding, and pressure >100 psig produced too fine a dust. Between these limits, grinding action generally increased nonlinearly with increased grinding air pressure. Figure 15 shows how air pressure affects the specific surface of the product. For the longer grinding times, doubling the pressure increased the specific surface by a factor of 5. Air pressure had much less effect on specific surface when the coal was milled very rapidly.

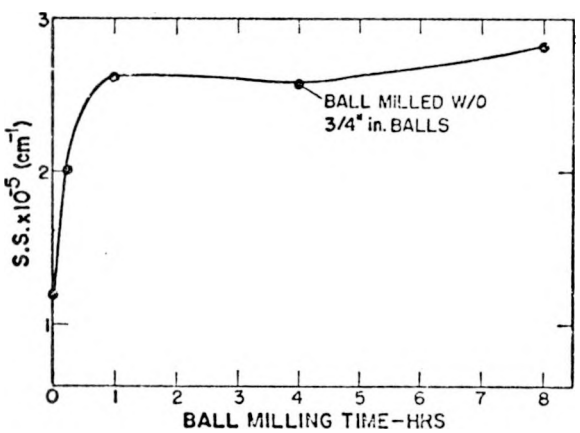

Fig. 14.
Ball milling effect measured by specific surface of coal dust.

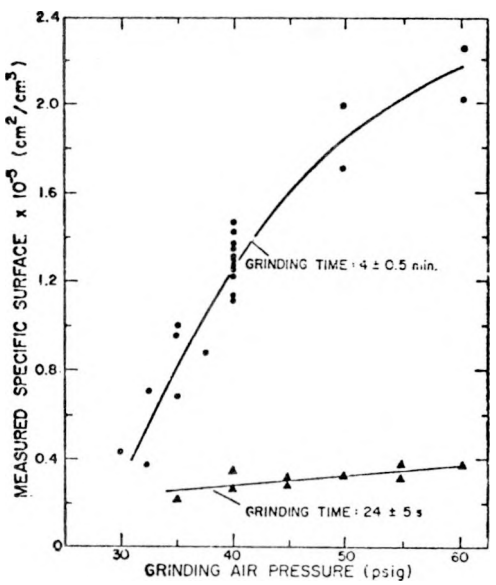

Fig. 15.
Specific surface of coal dust as a function of Micronizer air pressure.

Control of the grinding time was never completely satisfactory. Several devices for introducing coal into the Micronizer hopper at a uniform, controllable rate were evaluated. In one technique, the operator poured coal steadily onto a sloping metal tray that discharged into the hopper. Another feeder consisted of a vibrated cone or funnel with an outlet small enough to limit the powder flow to 100 g in 5 ± 0.5 min. A vertical standpipe taped to the conical Micronizer hopper, provided grinding times of 30 s or less. Because the standpipe was the same diameter as the top of the hopper and coal was rapidly dumped in to form a powder head, or column, this arrangement fed powder at a maximum rate. These feeders introduced 100 g of coal into the mill at rates varying from <30 s to >5 min. However, the reproducibility was no better than ±30 s, except for the standpipe. This feeder introduced coal in 25 ± 10 s, and produced a very coarse product. This is illustrated in Fig. 16 which shows specific surface as a function of milling time. Very short milling time, achieved with the standpipe feeder, produced powder with low specific surface. Low air pressure (<40 psig) likewise produced little size reduction. Because the constant pressure slope was small, making the grinding time less critical, 40 psig was chosen as the optimum grinding pressure.

In addition to changing the product size distribution, the various feeders produced a wide range of product recovery from the milling. Approximately 50% of the starting coal was recovered when milling times exceeded 3 min. However, as the milling time for 100 g of coal was decreased below 3 min, recoveries increased sharply. At 25-s milling time recovery was ~90%.

The Micronizer product showed no tendency to agglomerate either immediately after grinding or after storage. In view of this fact and the agglomeration problems of ball-milled coal dust, ball milling was abandoned in favor of fluid energy milling.

2. Specific Surface of Bulk Powders. The test dust required reproducible particle size characteristics from batch to batch. Therefore, it was necessary to monitor and control size distribution parameters to specified tolerances. Monitoring these parameters by standard methods (microscope, sedimentation, etc.) would have been time-consuming and expensive. Thus, surface area measurement was selected as a quality control method. Specific surface can be determined rapidly and inexpensively, although it does not define any one particle size distribution uniquely (i.e., two powders with the same surface area may have different particle size distributions). However, when one material is ground under controlled conditions, it is unlikely that two powder samples will have the same specific surface and markedly different size distributions. Therefore, under the above limitations, specific surface can be related to size distribution. Changes in specific surface will accompany changes in bulk powder size distribution parameters.

In principle, specific surface is an unambiguous property of any group of particles. It is defined as the surface area per gram, or per cubic centimeter. In practice, the specific surface of a particle or group of particles must be defined if pores form part of the surface, or if internal closed porosity contributes to the surface area. These definitions are reflected in the different methods of measuring surface area. For example, the B.E.T. nitrogen adsorption method[16] is a well-known method that includes open porosity in the results. Another method used extensively for quality control in producing many powders is the air permeability, or permeametry, technique. Only the external particle features contribute to this measurement. It is essentially a measure of aerodynamic drag on a powder compact. Thus, the value obtained can be related to the aerodynamic diameter of the particles. The air permeability method was chosen to monitor size distribution parameters because of its simplicity and rapidity. Carman and Malherbe's technique for measuring the surface of cement[17] was selected because the calculations include a slip factor term that makes the equation applicable to <2-μm particles. Unfortunately, these formulae contain empirical constants (as do most permeability equations) that prevent direct

correlation with other surface area techniques. Thus, the technique is most useful and precise for comparing separate portions of the same powder.

Calculation of specific surface from permeability data is based upon the Carman-Kozeny equation as modified by Arnell and Carman.[18]

$$\frac{Q_1 L P_1}{tA\Delta P} = \frac{P_m F_1}{5 \eta S_0^2} + \frac{0.96 F_2}{S_0}\sqrt{\frac{RT}{M}} , \qquad (1)$$

where

Q_1 = volume of air passed through plug, cm³,
L = length of sample plug, cm,
P_1 = barometric pressure in cm Hg,
t = time required to pass air volume Q_1 through plug, s,
A = face area of plug, cm²,
P_m = average pressure within compact, cm Hg,
ΔP = pressure drop across compact, cm Hg,

$F_1 = \frac{\epsilon^3}{(1 - \epsilon)^2}$ (Kozeny porosity function),

ϵ = compact porosity,
η = dynamic viscosity of air, stokes,

$F_2 = \frac{\epsilon^2}{(1 - \epsilon)}$ (Knudson flow porosity function),

R = gas constant, (8.31×10^7 in cgs units),
T = temperature in degrees Kelvin,
M = molecular weight (air),
S_o = specific surface in cm²/cm³.

The Carman-Kozeny equation can be reduced to the following explicit form.

$$S_0 = \frac{S_m}{2} + \sqrt{\frac{S_m^2}{4} + S_K^2} , \qquad (2)$$

where

$$S_m = \frac{tA\Delta P}{Q_1 LP_1} \cdot 0.96 F_2 \sqrt{\frac{RT}{M}} \text{ and } S_K^2 = \frac{tA\Delta P}{Q_1 LP_1} \frac{F_1 P}{5\eta} .$$

S_m is the slip or Knudson flow contribution to the surface area and S_K is the viscous flow contribution. For particles >3 μm, S_m becomes very small, whereas for smaller particles, it becomes appreciable.

The calculations are simplified, and, in practice, precision is improved by using constant sample weight, volume, and porosity. If, in addition, the same air volume is passed through each sample and the temperature, barometric pressure, and pressure difference are held constant the calculations involve only one independent variable, time.

The air permeability apparatus, adapted from that of Carman and Malherbe, is shown in Fig. 17. The sample is prepared by pressing a constant weight of coal dust to fixed plug dimensions. The sample holder A is sealed into the top of the volumetric burette, and pressure is reduced at the top of the plug. While valve C is open, pressure in the burette is unaffected, but when it is closed the flow of air through the plug reduces the pressure as indicated by manometer D. To maintain atmospheric pressure in the burette, air is admitted through valve J forcing liquid into the burette to restore atmospheric pressure. Thus, the volume of air flowing through the sample because of its pressure difference is continuously balanced by the volume flow of liquid into the burette. The time required to fill the burette with a predetermined volume of liquid is measured. This time and the barometric pressure, along with the other preset parameters, suffice for calculating specific surface.

Specific surface measurements made at different pressure drops across the compact generally disagree and indicate a surface increase with increased $\triangle P$. Figure 18 illustrates this effect for samples of differing porosity. The abscissa, P_m, is equal to $P_1 - \triangle P/2$ and indicates the average pressure, assuming a linear decrease through the compact. This phenomenon is due to the use of mean pressure in the calculations, rather than the true pressure distribution across the sample. Therefore, specific surface is normally measured and calculated for only one pressure difference. The $\triangle P$ chosen for our surface measurements was 200 torr which produces a mean pressure of 480 torr at local average barometric pressure of 580 torr. Because apparent specific surface vs mean

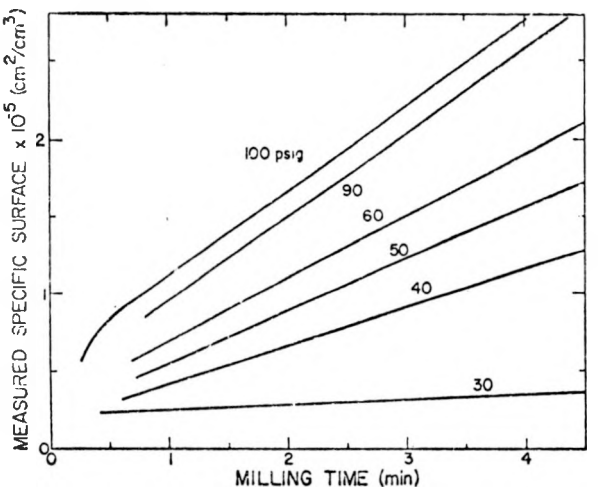

Fig. 16.
Specific surface of coal dust as a function of milling time.

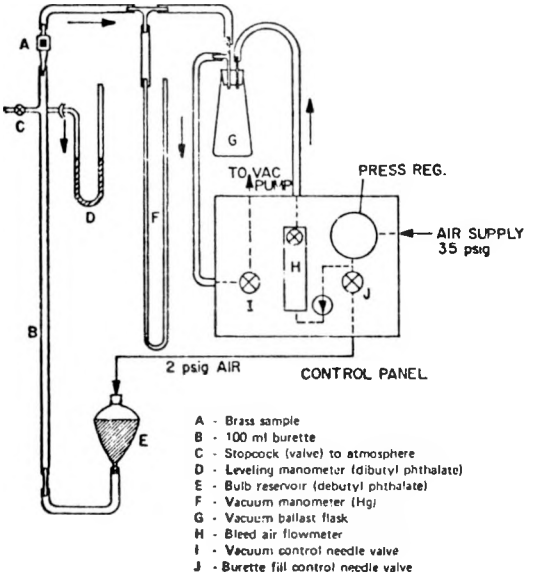

Fig. 17.
Specific surface measuring apparatus.

pressure (Fig. 18) tends to level off at high mean pressures, the mean pressure used should be as high as possible. However, high mean pressure required small pressure drop across the compact, producing in turn, an impractically long determination time for each determination. As a compromise, 200-torr pressure difference across the compact (P_m = 480) gave a determination time of 1 to 10 min.

Porosity of the sample compact is a critical parameter in the Carman-Kozeny equation. The porosity is equal to the void fraction of the compact and is defined by $\epsilon = 1 - \rho V/W$, where ρ = particle density, V = volume of compact, and W = mass of powder. In the functions F_1 and F_2, the porosity, ϵ, is raised to the third and second powers, respectively. This makes the measured specific surface sensitive to porosity. Moreover, experiment showed that the apparent specific surface of coal dust increases more with decreasing porosity than the porosity functions predicted. This may be due to de-agglomeration of particles, changes in pore size distribution, or crushing of particles by high compaction pressure. As a consequence, the porosity range of 0.4 - 0.5 void fraction appeared most valid for surface measurement. In this porosity range, most agglomerates have been broken and particle-to-particle contact occurs. Compression to lower porosities often requires considerable energy and causes crushed particles. Some powders exhibit an apparent specific surface vs porosity plateau in the void fraction range of 0.4 to 0.5. However, the coal dust tested showed very little plateau (Fig. 19). A porosity of 0.45, in the region of least slope, was selected for use in our experiments.

3. Density. An air-helium comparison pycnometer provided bulk density measurements of the milled coal. This device compares the volume of a sample chamber, first empty and then filled with coal dust, to a known volume. The dust volume together with the dust mass provides a measure of the bulk density. The density of the test coal dust was 1.32 ± .05 g/m³.

4. Bulk Dust Size Distribution. The size distribution of selected batches of milled coal was measured by transmission EM. Two sample-mounting methods were used.

The C-N mounting method[19] was used initially. Briefly, it consists of mixing the coal sample into a 60 wt.% camphor-40 wt.% naphthalene eutectic (C-N), placing a droplet on an EM grid,

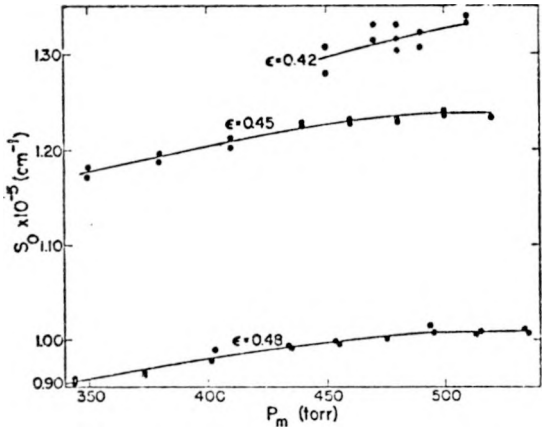

Fig. 18.
Apparent specific surface of coal dust as a function of mean compact pressure.

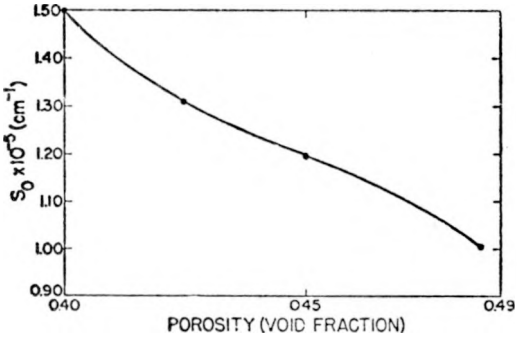

Fig. 19.
Apparent specific surface of coal dust as a function of compact porosity.

cooling below 32°C to solidify the eutectic, and subsequently evaporating the eutectic from the in-place particles. This is followed by the usual shadowing procedure.

Later, LASL developed a simple, precise method for mounting the bulk dust.[20] An aqueous suspension of coal dust particles is filtered through a 0.8-μm pore size Millipore AA filter. The filter containing the dispersed particles is fused, coated with carbon and chromium, and dissolved by an acetone vapor process. After this the remaining carbon-chromium film containing the particles is inverted for final chromium shadowing.

The coal dust was photographed at magnifications of 2000-3000 X. Enlarged particle images were sized on a Zeiss TGZ-3 comparator. Size distributions were computed and graphed, using the midpoint of the Zeiss size intervals for each group diameter.

5. Air Dispersion Techniques. Micronized dusts from the milling experiments were dispersed in air to measure airborne size distribution. Regardless of the bulk powder size distribution and uniformity, consistent dispersion with a reproducible size distribution is required. Less critical, but important, is uniform dust concentration. However, the dispersion at a constant rate or concentration is difficult, and concentration variation <10% is uncommon.

The original air dispersion system used in these experiments consisted of a WDF mechanism and other components similar to those used in the small aerosol test system described in Sec. I. These components were not housed in a single cabinet, as was the SIC system, but were arranged on a bench top.

Dusts to be dispersed were pressed into the 0.5-in.-diam WDF cup by a hydraulic press. Pressing loads varied from 358 to 717 kg/cm^2 (5100 to 10,200 psi) according to the specific surface of the coal dust. Dusts with high specific surface required lower pressures than did coarse dusts. The properties desired of a compact were good mechanical integrity, no surface erosion by the carrier air, little particle agglomeration due to pressing, and uniform strength and density.

The suspended dust passed through a 4-Ci tritium charge neutralizer. Subsequent investigation indicated less activity was sufficient to neutralize the particles (see Appendix); consequently, the 4 Ci tritium neutralizer was replaced by one with 200 mCi tritium.

Beyond the neutralizer, the aerosol entered the aerosol chamber through a dilution and mixer device. Both the chamber and the dilution and mixer were as described in Sec. I. All samples taken during dust development were withdrawn through the ports around the cylinder wall or those in the plexiglass chamber lid.

6. Size Distribution Measurement Techniques. Instruments investigated for determination of aerodynamic size characteristics were an AI,[21] Andersen mini-impactor,[22] and the Lovelace Aerosol Particle Separator (LAPS).[23] The 10-mm nylon cyclone also was used to provide a size estimate.

The AI provided the most reliable size information. Operated at 28.3-ℓ/min (1-cfm) airflow, it collected enough dust on 81-mm-diam membrane filter impaction surfaces to give good mass sensitivity in a reasonable time.

Two Andersen mini-impactors, one a LASL modification of the commercial instrument, provided size data which agreed fairly well with that from the six-stage AI, but their mass sensitivity was relatively poor. Generally, the mass of dust collected was only 0.1% of the mass of the stage upon which it was collected and weighed.

Two-stage, 10-mm nylon personal samplers were also used in estimating the MMAD of coal dust clouds. If σ_g is assumed to correspond to the AI data, and total mass entering the cyclone is estimated using other data (membrane filters, total mass collected in aerodynamic samplers, etc.), the respirable fraction passing the cyclone filter can be found by gravimetric measurement

of total dust and dust on the personal sampler second-stage filter. Knowing the respirable mass (% passing the cyclone) and σ_g, one can estimate aerosol MMAD from parametric curves of cyclone filter efficiency as a function of MMAD and σ_g (Fig. 12). Generally, estimates made by this method were smaller than those from direct sampling techniques.

The LAPS was used during several sampling runs to determine the coal dust aerodynamic size distribution (Fig. 20). It is a centrifugal elutriation spectrometer that rotated at 1750 rpm in these experiments. The dust is distributed according to aerodynamic particle diameter along a metal foil collection surface that lines the 44-cm spiral channel length. After each run, 2-cm-long segments were cut from the foil deposition surface at selected intervals. These segments were weighed, sonically cleaned for a prescribed period, dried, and reweighed. The measured distribution of mass along the foil, along with the instrument calibration then defined the aerosol aerodynamic particle size distribution. This procedure was repeated using 25-mm-diam membrane filters as the collecting surfaces. Preweighed filters were affixed to the copper foil with ethanol, with 3 cm between filter centers. The filters were easily removed from the foil and weighed after each run. Although these techniques provided a good analysis of the deposited material, the accuracy suffered because inlet losses were significant and the laminar flow pattern near the exit filter was distorted. The latter situation was improved by removing the final filter from the channel and placing a membrane filter in the exhaust air line outside the head. Elimination of the filter in the channel improved the particle deposition pattern in this region. Inlet loss in LAPS averaged about 10% of the total mass collected during a run, as determined from washings. This loss was acceptable if the particle size distribution was not biased. However, the loss involved large particles exclusively, so the results always indicated a lower MMAD than other sizing devices.

Aerodynamic sizing of individual Micronized, dispersed dusts was done primarily using a six-stage AI with preweighed filters as collection surfaces on each stage. This instrument provided consistent aerodynamic sizing information. During initial sizing measurements, the glass fiber collection surfaces did not lie flat on the impaction surface and actually impeded airflow through many impactor jets. This caused excessive deposition on the impactor upper stages and a distribution biased toward a larger particle size. These 81-mm-glass fiber filters had been substituted for membrane filters whose weight seemed unstable. However, after glass filters proved unsuitable, membrane filter weight was found to be stable after 24-h exposure to ambient humidity and temperature. The possibility of bounce and re-entrainment of large particles was evaluated by using membranes covered with petroleum jelly on the first two stages. The size distribution was the same with or without petroleum jelly, indicating that little bounce or re-entrainment occurred. Airflow through the impactor was calibrated using a dry test meter immediately before and after each impactor sampling period. Generally, at least three separate 20- or 30-min impactor samples were collected in each 8-h dispersion run. Total mass concentration calculated from the impactor sample was generally <10% below the concentration measured by the membrane filter. When measurement errors such as wall deposition, sampling line loss, and some impaction of very large particles at the inlet are considered, this loss in the AI is not unreasonable.

Coal aerosol samples were collected by electrostatic precipitator for sizing by electron microscopy. The particles were collected on EM grids with carbon substrates, shadowed at a 30° angle with chromium, and photographed at a magnification of 3000 X. Particle images were then sized on a Zeiss TGZ-3 optical comparator measuring protected area diameters. Size distributions were curve fitted using a CDC-6600 computer.

D. Discussion and Results

Coal dust aerosols were produced using bulk dust specific surface to determine conditions required to produce an aerosol in the desired particle size range. A Micronized dust with known specific surface was dispersed, the size distribution measured, and the measured specific surface plotted vs the median size. The specific surface that gave a MMAD of 3.5 to 4.0 μm was found to be 1.1 - 1.2 x 10^5 cm^2/cm^3. Later, the coal dust shape factor, determined through use of the LAPS and photomicrography provided a means for calculating the specific surface of the dust using the Hatch and Choate equation.[24]

1. Milling and Specific Surface Correlation. Although grinding control was not sufficient to attain the specific surface wanted, Micronized batches were generally within ±10% of the the desired particle specific surface. However, blending two or more batches of dust to get a mix with desired size distribution proved feasible and made accurate grinding control less essential. Theoretically, blending two log-normally distributed dusts produces a bimodally distributed dust, but if the particle size distributions of the blending dusts do not differ widely, the mix approximates a log-normal distribution.

Specific surface measurements provided essential information about the relative size distribution of Micronized bulk dust with a precision of ±5% at the 98% confidence level. The reliability and accuracy of these results permit mixing two or more batches of dust to achieve a blended dust whose measured specific surface is within 3% of that desired.

2. Correlation of Specific Surface and Particle Size Distribution. The specific surface of the coal aerosol was calculated from particle size parameters and compared to that measured by the air permeability technique. The Hatch and Choate equation[24] relates specific surface to specific surface shape factor, density, count median diameter, and σ_g.

$$\ln S = \ln \frac{\alpha}{\rho \nu} - \ln (CMD) - 2.5 \ln^2 \sigma_g, \tag{3}$$

where

S = specific surface, (cm^2/g),
ρ = particle density, (g/cm^3),
$\frac{\alpha}{\nu}$ = specific surface shape factor,
CMD = count median diameter, (cm),
σ_g = geometric standard deviation.

To equate surface and size distribution one must know the specific surface shape factor (α/υ) in addition to the size parameters. Initially, α/υ from Kotrappa's results[25] was used in this equation. Later, size data from experiments with the LASL spiral centrifuge and the LAPS along with electron microscope sizing provided a basis for estimating the shape factor of the test coal dust. These data were not consistent, but they generally gave a coal dust surface area shape factor like Kotrappa's. Using α/υ = 31.1 and ρ = 1.32 g/cm^3, the specific surface of eight aerosols was calculated and plotted vs their measured specific surface in Fig. 21. Most of the data used to calculate the values shown were obtained from aerodynamic particle sizing, but specific surface calculated from bulk dust samples and ESP samples is included.

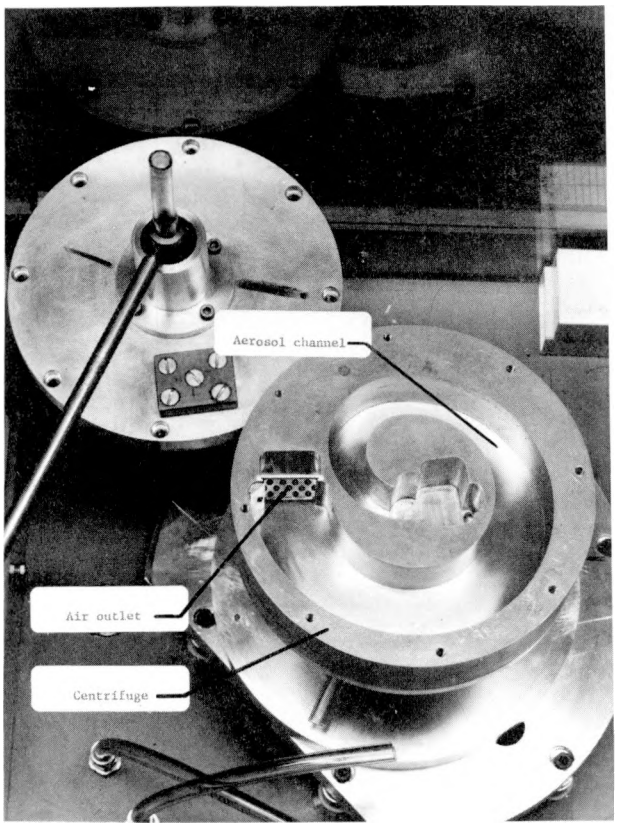

Fig. 20.
Lovelace Aerosol Particle Separator (LAPS), exploded view.

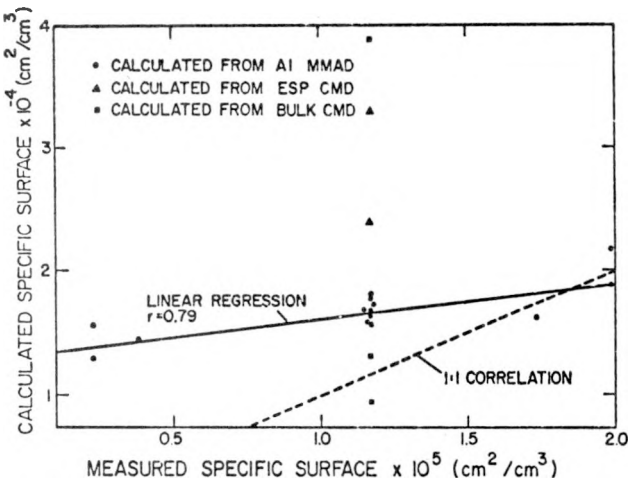

Fig. 21.
Calculated vs measured specific surface correlation.

Normally, to use MMAD to calculate specific surface, one must know a dynamic shape factor, κ. The MMAD can then be used with κ and ρ to calculate a mass median diameter (MMD). Finally, the MMD is converted to CMD which may be used in the Hatch and Choate equation to calculate the specific surface. LASL, however, used Kotrappa's ratio MMAD/MMD = 1.02 for coal dust. As this ratio was determined experimentally, it includes correction for both ρ and κ.

When measured specific surface is plotted vs calculated specific surface (converted to cm^2/cm^3) a line with slope of 1 should be obtained if the air permeability method correlates identically with the size parameters. However, in Fig. 21, the calculated specific surface is a fac ~ of 5 less than the measured specific surface for all dusts.

The discrepancy between measured and calculated specific surface and the scatter in calculated specific surface may be attributed to several things. The variation in measured specific surface of bulk Micronized coal was slight, whereas the calculated specific surface based on size characteristics of the coal aerosol varied considerably. Calculated specific surface is obtained by substituting aerosol CMD and σ_g, determined from electron micrographs, into the Hatch and Choate equation. Because σ_g can have ±10% error, the term 2.5. $\ln^2 \sigma_g$ in this equation may produce a ±40% variation in calculated specified surface. The coal dust specific surface shape factor may have as much as 50% error.

Another factor that may account for a major part of dust discrepancy between measured and calculated specific surface is the possibility that the particle size distribution of air-dispersed dust differs from that of the bulk dust owing to losses, shattering, agglomeration, etc., during dispersion. A review of aerodynamic and microscopic sizing and specific surface measurements indicated that although the bulk powder dispersed was increasingly coarsened, the airborne dust size parameters changed little.Thus, as the specific surface of bulk dust decreased by a factor of

4, the MMAD of the airborne dust increased by only 15%. This suggested that part of the large particles were not reaching the aerosol chamber. In two experiments, the de-agglomeration baffle was removed from the WDF exit. Then two dusts that had been previously dispersed with the baffle in place were redispersed. The particle size parameters changed significantly (Table IV) in one case, but whether this change is due to increased agglomerates in the cloud or to an actual increase in the number of large particles is not clear. Probably both mechanisms contribute to the greater MMAD when the baffle is removed from the WDF.

E. Conclusion

LASL has developed a standard test coal dust under an Interagency Agreement between NIOSH and ERDA. Coal dust provides a well-characterized, realistic cloud for checking performance of personal coal mine air samplers. Figure 22 outlines the steps in development and production of this standard coal dust. This diagram includes the major information feedback loops such as the specific surface and size distribution correlation.

Test dust particle size parameters were selected by considering the theoretical separation of a log-normally distributed, polydisperse dust by an ideal cyclone as defined by Moss[14] and Lynch.[15] Their results show that a polydisperse dust of 3.75-μm MMAD will be 46% respirable as defined by the ACGIH curve[6] regardless of its dispersity (σ_g), if it has a log-normal size distribution. Therefore, a standard dust with 3.75-μm MMAD and $\sigma_g \geq 2.0$ was the goal.

The test coal dust was produced from Pennsylvania bituminous, lower Kitanning seam coal. Batches of 100 g of powder were ground in a Micronizer fluid energy mill to the desired size distribution as indicated by a measured specific surface. Aerodynamic particle size distribution of the dispersed dust was measured using a six-stage AI. Production of consistent dust size parameters requires standardized operation of the generating system.

The test dust properties were:

MMAD = 3.8 ± 0.25 μm and σ_g = 2.1 ± 0.1 based on 25 samples.

Density = 1.32 ± 0.05 g/cm^3 measured with an air and helium comparison pycnometer.

Specific Surface = 1.16 ± 0.06 x 10^5 cm^2/cm^3 measured by air permeability at 0.42 void fraction.

The aerosol size parameters are like those reported in many coal mining operations, and small changes in the aerosol produced during each test run cause minimal change in the respirable fraction. The dust was blended from 25 separate Micronized batches whose specific surface measurements were used to predict the characteristics of the resultant composite bulk dust. Use of specific surface to monitor the final bulk dust proved successful, and specific surface was within ±5% of that estimated from specific surface measurements of the individual batches before blending.

This standard test dust permits evaluating the performance of coal mine air samplers with ±10% accuracy. It can be used as a single point calibration for the 10-mm nylon cyclone, or the MRE horizontal elutriator, and to evaluate the relative performance of sampling systems used, or proposed for use, in coal mines.

IV. COAL DUST STUDIES

During and after development of the hardware and standard dust, the performance of coal dust air samplers and associated filtration media was investigated. Some work was necessary to define characteristics of the aerosol test systems and standard dust in conditions not anticipated in their design. Other work with personal coal mine air samplers and aerodynamic particle sizing instruments was performed to measure their performance when sampling coal dust clouds. Of interest were prolonged (12-h) operation of personal samplers in moderately dusty environments

TABLE IV

PARTICLE SIZE CHARACTERISTICS OF SUSPENDED COAL DUST GENERATED BY THE WDF

Dust	Size Parameters		
	CMD[b] (μm)	σ_g	MMAD[c] (μm)
M-17	0.40 ± 0.04	2.09 ± 0.18	3.5 ± 1.4
M-17[a]	0.53 ± 0.03	1.99 ± 0.16	3.6 ± 0.8
M-41	0.54 ± 0.01	1.91 ± 0.01	2.8 ± 0.3
M-41[a]	0.61 ± 0.07	2.00 ± 0.08	4.8 ± 0.4

[a]Dispersed from WDF with deagglomeration plate removed.

[b]Average of at least two ESP-electron microscope sizing samples.

[c]Average MMAD from five aerodynamic particle size-measuring instruments.

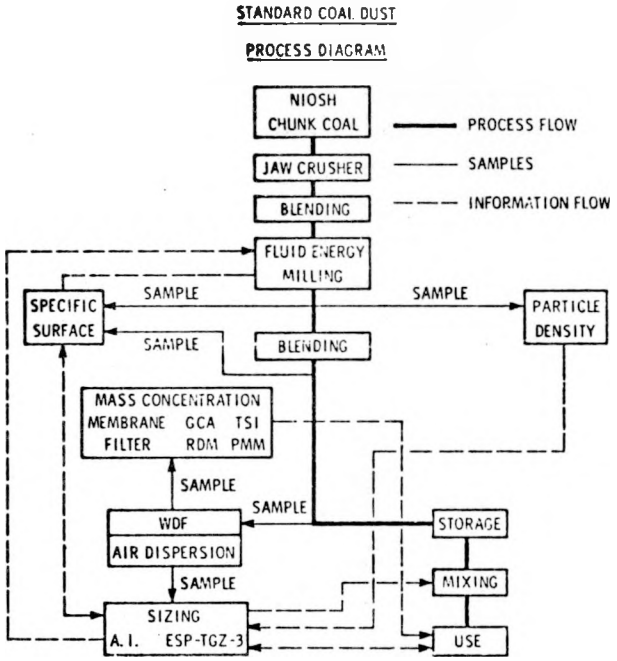

Fig. 22.

Coal dust development program.

the effect of second-stage filter efficiency, and any effect of dust cloud electric charge on the collection characteristics of the cyclone presampler in low relative humidity environments. These studies used the SIC System, standard coal dust, and other log-normally distributed coal dusts.

A. Cyclone Calibration

Previous calibrations of the 10-mm nylon cyclone[3-5] with monodisperse aerosols indicated flow rates ranging from 1.4 to 2.0 ℓ/min were required to match the ACGIH respirable dust criteria. Two investigations[26,27] using polydisperse coal dust indicated flow rates of 1.7 and 2.0 ℓ/min, respectively. The several well-characterized, log-normally distributed dusts produced by Micronizer milling the Pennsylvania coal were used to further calibrate this cyclone.

Polydisperse coal dusts were used to calibrate 10-mm nylon cyclone samplers operated at flow rates of 1.7 and 2.0 ℓ/min. Four personal samplers and three membrane filter total dust samplers were suspended in the SIC aerosol chamber for each run. The desired flow rate was controlled at ±3% by critical orifices. During each 8-h experiment, the personal samplers were operated for three 45-min periods and at least three total dust samples were collected during each period. Twenty-minute AI samples were obtained 1 h before each personal sampler operating period. These were collected on 81-mm-diam Gelman DM-800 membrane filter surfaces on each stage of the six-stage samplers. A final 47-mm-diam Gelman DM-800 filter collected the finest particles. The MMADs of the test aerosols were 2.8, 3.3, 3.7, 4.5, and 5.2 μm with σ_g ranging from 1.7 to 2.6. Gross dust concentration was approximately 4 mg/m³ in each experiment, thus roughly 100 μg of the coarsest dust (5.2 μm) was collected. The microbalance used to analyze the second-stage filters had a precision of ±5 μg and the estimated accuracy of the procedure was ±10 μg. Thus the maximum relative error in the personal sampler penetration measurements was about 10%.

The accuracy of the particle size distribution measurements was slightly better, because the minimum amount of dust collected per stage was almost 200 μg. However, the error was larger than the 5% this weight would indicate, because the weight stability of the 81-mm-diam filters was less than that of the smaller personal sampler second-stage filters.

Calibration curves from these tests are shown in Fig. 23. Each data point represents one experimental run, or 8 to 12 personal sampler penetration determinations and three AI determinations. The dashed curve is the ACGIH respirable dust curve corrected for polydispersity by using Moss's[14] numerical polynomial curve-fitting results. The abscissa also indicates σ_g for each particular MMAD. Consequently, both size parameters (MMAD and σ_g) can be read for each dust (data point), as well as for any point on the adjusted ACGIH curve. Of course, this calibration applies only to log-normally distributed dusts, but all Micronized dusts closely approximated such distributions.

The calibration results indicate that the 10-mm-nylon cyclone operated at a flow rate of 1.7 ℓ/min defines a respirable fraction in reasonable agreement with the ACGIH curve. However, the cyclone particle size separation curve is steeper than the ACGIH respirable dust curve. This is indicated by the consistently higher measured respirable fraction at <4-μm MMAD and generally lower fraction at >5-μm MMAD. The calibration curve indicates that the cyclone operated at 1.7 ℓ/min overestimates the respirable concentration of <4-μm dusts and gives an underestimate of that of coarser dusts. At 2-ℓ/min flow, the cyclone apparently underestimates the respirable dust concentration throughout the size range of this calibration.

An explanation of the change in σ_g as MMAD changes in Fig. 23 is in order. The Micronizer mill used to produce all the coal dusts is not only a comminution device, it also contains a classifier (cyclone) to separate product dust from the air. As product size, milling air pressure, and other variables change, so does the separation efficiency. As the median diameter of the product increases, less product exhausts with the cyclone effluent, and the polydispersity of the product increases.

B. Loading Effects

The effect of loading on the cyclone personal air sampler estimates of respirable dust concentrations was examined. Personal coal mine air samplers with both VM-1 and FWS-B second-stage filters were tested by sampling a coal aerosol for up to 21 h at an initial flow rate of 2 ℓ/min. This flow rate was selected because it is used in coal mine air sampling, and also should produce more pronounced mass loading effects than a flow of 1.7 ℓ/min. Second-stage filters were changed every 7 h or less to prevent excessive filter loading and to correspond to present mine-sampling practice. The cyclones were operated up to 21 h without cleaning. Both Gelman VM-1 and MSA FWS-B, 5-μm pore-size, membrane filters in 37-mm-diam cassettes were used as second-stage collectors. During each 7-h period two additional personal samplers were operated for three or four 45-min periods to measure the respirable fraction over short time intervals. Gross dust concentration, also measured with membrane filters, was ~4.0 mg/m^3. This provided a respirable dust concentration of 1.8 mg/m^3. The standard coal dust used as the test aerosol and the SIC aerosol test system are described in Secs. II and III.

Cyclone loading decreases the respirable dust estimate slightly for sampling times of up to 7 h. Figure 24 shows the ratio of the respirable coal dust fraction measured over long periods to the respirable fraction measured by short-term sampling. This penetration ratio (P.R.) puts all measurements on the same basis so that all runs may be compared. Loading does not affect the short-term (45-min) samples. For each 7-h period in Fig. 24, a linear penetration decrease is shown for simplicity. The personal sampler loading characteristics were defined by connecting the data points at 7-, 14-, and 21-h total cyclone operation. However, because the second-stage

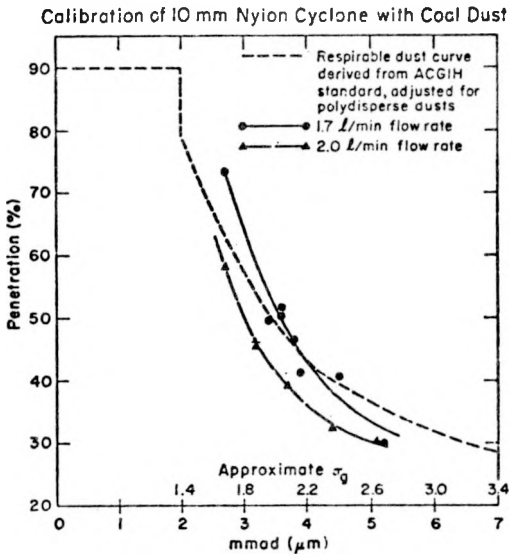

Fig. 23.
Separation efficiency of coal mine personal sampler at 1.7- and 2.0-ℓ/min flow rates.

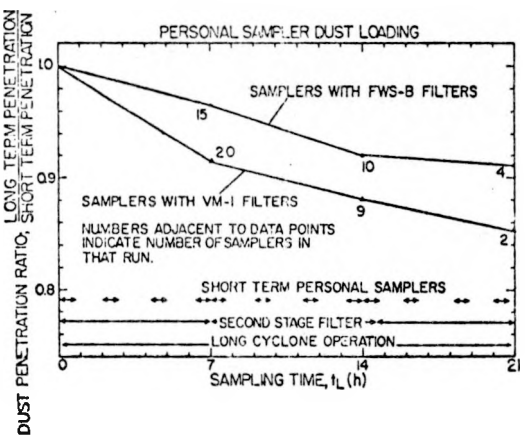

Fig. 24.
Loading effects in personal samplers equipped with FWS-B and VM-1 second-stage filters.

filters were changed every 7 h, the loading could be separated into parallel, sloping line segments with an initial P.R. of 1.0 if no cyclone loading occurred. Instead, the data points continue downward with time, indicating additional loading because the cyclone body was not cleaned for 21 h. That the lines for the two types of second-stage filter do not coincide indicates an effect due to differences in filtration characteristics.

The effect of loading on respirable dust estimates can be illustrated by considering a typical sample situation. Consider a personal sampler operating 7 h at 2-ℓ/min flow rate, sampling a coal aerosol of 4-mg/m³ mass concentration with log-normal particle size distribution parameters of 3.7-μm MMAD and σ_g of 2.1. After 7 h of operation under these conditions, the dust analysis is as summarized in Table V for various degrees of realism and no sampling errors. Each row of the table shows the results expected from a particular sampler. A filter sampler operating in the specified dust cloud at 2.0 ℓ/min would collect 3360 μg of dust. An ideal respirable dust sampler operating in accordance with ACGIH criteria would collect 1562 μg and indicate a respirable dust concentration of 1.86 μg/ℓ. A LASL calibrated cyclone and filter assembly exhibiting no loading effects and operated at 2.0 ℓ/min would indicate a respirable mass concentration of 1.56 μg/ℓ (Row 3). Results from similarly calibrated cyclones including loading effects, determined from Fig. 24 would be 1.51 and 1.43 μg/ℓ depending on the second-stage filter (Rows 4 and 5). For example, a cyclone operated at 2 ℓ/min with a FWS-B second-stage filter (Row 4) will show an apparent 37.7% penetration in a 7-h sampling period. This is given by

$$P = \frac{(0.966)(1310\ \mu g)}{(3360\ \mu g)} \cdot 100 = 37.7\% \ .$$

The apparent respirable dust concentration (1.51 μg/ℓ) is then determined by dividing the collected dust mass (0.377 x 3360 = 1267 μg) by the anticipated sample volume (2 ℓ/min times 420 min). This respirable dust concentration is 19% lower than the ideal (ACGIH) concentration, as shown in column 8.

A personal sampler operating at 2.0 ℓ/min without loading should collect 1310 μg of respirable dust on its second-stage filter in 7 h. This is a respirable dust concentration of 1.56 μg/ℓ, 16% below the concentration given by the ACGIH curve. If the sampler operates realistically (loads with time), second-stage collection, using a VM-1 filter, is as much as 23% lower than the ACGIH value.

A similar analysis of personal samplers operating at 1.7 ℓ/min is also presented in Table V. At this flow rate, some assumptions were necessary as experimental loading data were not obtained. First, total loading is assumed proportional to total mass passing through the sampler; second, it is assumed equal at 1.7 and 2.0 ℓ/min, given equivalent total dust entering the cyclone. The first assumption is based on the belief that filter loading depends on the amount of dust collected, not on the collection rate. The second assumption is only an approximation since, at 1.7 ℓ/min, a higher proportion of the mass is deposited on the second stage. On the basis of these assumptions, a sampler operating at 1.7 ℓ/min loads as much in 7 h as one operating at 2.0 ℓ/min loads in $\frac{1.7}{2.0} \times 7 \simeq 6$ h. Therefore, the P.R.s are taken from the loading curves in Fig. 24 at a time of 6 h.

The advantage of using the lower flow rate is emphasized by column 5 of Table V. Because the calibrated penetration for operation at 1.7 ℓ/min overestimates the respirable dust (48% on the second-stage filter vs 46.5% theoretically respirable), and the loading is less than that at 2-ℓ/min flow, a sampler operated at 1.7 ℓ/min will provide an estimate very close to the ACGIH value.

The effects of loading by aerosols of other sizes may be estimated from this analysis and the dust calibration curve (Fig. 23). At 2.0-ℓ/min flow rate, loading that decreases the mass collected on the second-stage filter can only increase the error in the respirable dust estimate. This is because the penetration curve at this flow rate is already below the ACGIH curve, so loading increases the underestimate. On the other hand, at 1.7 ℓ/min and for MMADs less than ~4 μm, loading may improve the respirable dust estimate during long-term operation. Here, the greater cyclone penetration due to small MMAD is balanced by decreased flow due to loading. Loading causes a net decrease in second-stage collection, and the resulting lower respirable fraction compensates for the disagreement with the ACGIH respirable dust curve value.

Wherever the calibrated penetration efficiency is less than that predicted by the ACGIH curve loading will increase the underestimate of respirable dust. However, in this case, the second-stage filter loading will decrease as MMAD becomes larger, due to less penetration through the cyclone. Consequently, for long-term operation in coarse dusts (>4-μm MMAD), the error in estimated respirable fraction due to loading is probably not serious at either flow rate.

Further analysis of the experimental loading curve (Fig. 24) provides some insight into the loading mechanism. To examine each 7-h operation interval more closely, the loading curve with VM-1 second-stage filter is redrawn (Fig. 25) in separate 7-h intervals. Linear loading is assumed (only the end points of each interval are considered) by joining the starting point and the 7-h data point (segment V_1). Segments V_2 and V_3 for 14 and 21 h are constructed from the end points for those time intervals back to the starting time for those particular filters using the same slope as for V_1 because all filters should load similarly. Segments V_1, V_2, and V_3 represent total loading increments. The difference between the end points (v_{12}, v_{22}, v_{32}) and the dashed line defined by points v_{11}, v_{21}, and v_{31} represents filter loading, whereas the dashed line represents cyclone loading. The equation for the dashed line is P.R. = $1 - 0.0048t_L$.

Performing the same manipulations with the data from FWS-B filter-equipped personal samplers produces confusing loading lines. First, the overall loading curve (Fig. 24, upper line) is nearly linear for the entire 21-h sampling period, suggesting that only one mechanism is involved. Second, the slopes of the individual segments (Fig. 26) are identical to the slope of the best-fit straight line through the data, again indicating only one loading mode, cyclone loading. The equation for this dashed line is P.R. = $1 - 0.005t_L$, almost identical to that for cyclone loading determined from VM-1 data.

TABLE V

ERROR IN RESPIRABLE DUST ESTIMATE[a]

Sample No.	Flow Rate (ℓ/min)	Sampler	Penetration Ratio (Fig. 24)	Penetration (%)	Dust Mass (μg)	Apparent Respirable Dust Conc (μg/m³)	Error[b]
1	2.0	Total dust	---	---	3360[c]	---	---
2	2.0	Ideal (ACGIH)	---	46.5	1562	1.86	0
3	2.0	Calibrated Cyclone (No loading)	1	39.0	1310	1.56	-16
4	2.0	Calibrated Cyclone w/FWS-B (loading occurs)	0.97	37.7[d]	1267	1.51	-19
5	2.0	Calibrated Cyclone w/VM-1 (loading occurs)	0.92	35.7[d]	1199	1.43	-23
1′	1.7	Total dust	---	---	2856[c]	---	---
2′	1.7	Ideal (ACGIH)	---	46.5	1328	1.86	0
3′	1.7	Calibrated Cyclone (No loading)	1	48	1371	1.92	+3
4′	1.7	Calibrated Cyclone w/FWS-B (loading occurs)	0.97	46.6[d]	1331	1.86	0
5′	1.7	Calibrated Cyclone w/VM-1 (loading occurs)	0.93	44.6[d]	1275	1.79	-4

[a] 7-h operation, 4.0 mg/m³, log-normal size parameters: 3.7-μm MMAD, σ_g = 2.0.

[b] % error relative to ideal ACGIH respirable dust concentration.

[c] Total dust entering cyclone in 7 h at 4 μg/ℓ.

[d] Effective penetration after 7-h operation: product of column 3 and calibrated short-term penetration (39% at 2.0 ℓ/min, 48% at 1.7).

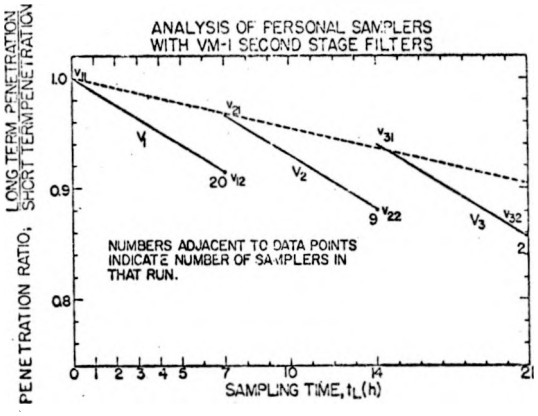

Fig. 25.

Reconstruction of loading effect in personal samplers equipped with VM-1 filters.

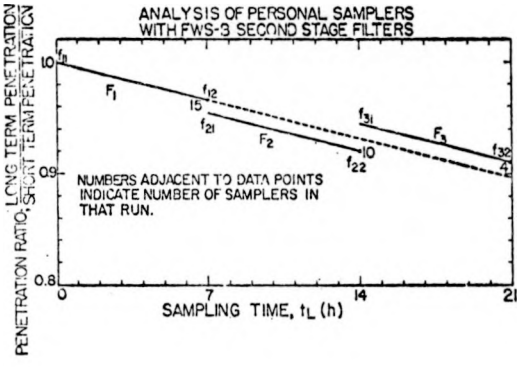

Fig. 26.

Reconstruction of loading effect in personal samplers equipped with FWS-B filters.

The physical mechanism for cyclone loading is unknown, but it may be the buildup of chain type agglomerates within the cyclone and their periodic detachment from the cyclone wall and deposition in the bottom of the cyclone collector well. On the other hand, we can hypothesize that the filter-loading effect is due to reduced flow through the personal sampler resulting from increased filter resistance. Credence is given to this hypothesis by the difference in performance of VM-1 and FWS-B filters, which presumably arises from their structural difference. The VM-1 filter has a uniform pore structure throughout, whereas the FWS-B has large pores (~50 μm) on its upstream face, decreasing to small ones (<5 μm) on the downstream face (Fig. 27). The filters also have visibly different collection characteristics. The VM-1 collected most of the coal on the upstream face, which became black, but the FWS-B collected much of the dust near its rear surface so that a gray upstream, and slightly darker downstream, face resulted. Thus, the FWS-B filter appears to collect throughout its thickness, whereas the VM-1 builds a high-resistance cake on its face.

C. Coal Dust Penetration Through 5-μm Pore-Size Filters

Because membrane filters with nominal 5-μm pore size are used routinely in industry to sample coal dusts, the efficiency of this sampling medium against coal dust and its respirable fraction was evaluated. Tests used 37-mm-diam, 5-μm-pore VM-1 and FWS-B filters at flow rates used in mine sampling.

Average total coal dust concentration determined using membrane filters was 4.3 $\mu g/\ell$, and two AI samples gave the aerosol MMAD as 3.4 μm with σ_g = 2.0. VM-1 and FWS-B filters were used to collect both total and respirable dust. The latter was defined by a 10-mm-diam nylon cyclone precollector operated at 2.0 ℓ/min, the standard in-mine sampling airflow. Each filter was backed by DM-800 (0.8-μm pore) filters, a GCA RDM, or the TSI PMM. Thus, the back-up collectors were challenged by the very small mass penetrating the membrane filters.

Table VI summarizes the data, showing that in the low dust concentrations downstream of the VM-1 or FWS-B filters the TSI PMM seems to function better than DM-800 filters or the GCA RDM. The DM-800 filters have moisture and charge problems, and the RDM is not sensitive enough at very low concentrations and small particle size to detect any material that passes the 5-μm filter. The large standard deviations emphasize the measurement techniques' poor sensitivity for this small mass and indicate that no significant difference between total and respirable dust penetration through the 5-μm filters can be inferred. Short-term penetration through the 5-μm membrane filters is ~1-2% by either this coal dust aerosol or its respirable fraction. This degree of penetration is not significant in assessing potential worker exposure to coal dust, because other variables inherent in field sampling are of greater consequence.

D. Coal Dust Aerosol Electric Charge and Its Effects on Sampler Performance

The effect of coal dust electric charge on the nylon cyclone personal sampler performance was studied. First, the particle size characteristics of charged and neutralized aerosols at low humidity were measured. Next, several systems were used to quantify the aerosol particle charge on the coal dust. Finally, experiments comparing cyclone performance in charged clouds confirmed other investigators'[11,13] findings that the nylon cyclones' separation characteristics were not affected by electrically charged dust clouds.

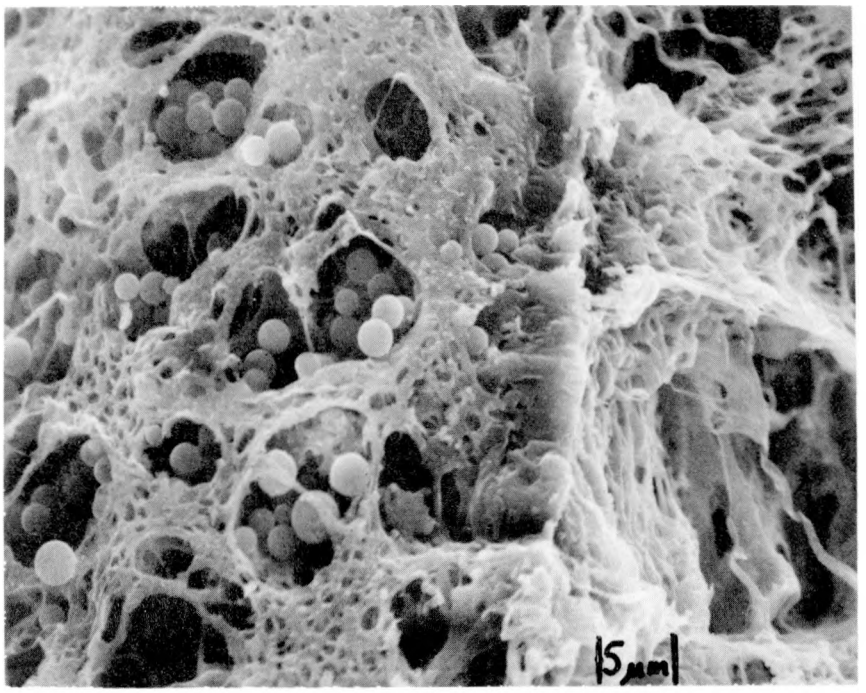

front VM-1 rear

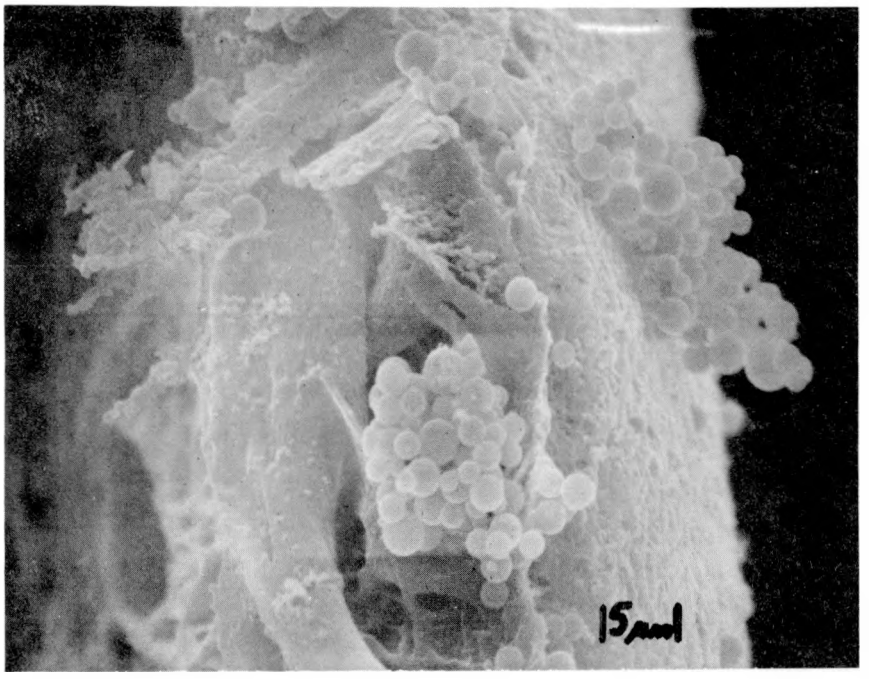

front FWS-B rear

Fig. 27.

VM-1 and FWS-B 5-μm pore size membrane filter structure in cross section.

TABLE VI

EFFICIENCY OF 5-μm MEMBRANE FILTERS AGAINST COAL DUST[a]

Dust	Sampling Time s	Sampling Time (min)	Filter	Mass Collected (μg)	Backup	Mass Collected (μg)	% Penetration
Total	720	(12)	VM-1	132	DM-800	-11	0
Total	1320	(22)	VM-1	168	RDM	---	0
Total	780	(13)	VM-1	117	PMM	1.4	1.2
Total	720	(12)	VM-1	111	DM-800	-2	0
Total	720	(12)	VM-1	123	DM-800	1	0.8
						Mean	0.4 ± .6
Total	720	(12)	FWS-B	112	DM-800	-5	0
Total	720	(12)	FWS-B	125	DM-800	5	4.0
						Mean	2.0 ± 2.7
Respirable[b]	2700	(45)	VM-1	173	DM-800	2	1.1
Respirable	2700	(45)	VM-1	182	DM-800	-1	0
Respirable	2700	(45)	VM-1	158	DM-800	8	4.9
Respirable	780	(13)	VM-1	62	PMM	1.0	1.7
						Mean	1.9 ± 2.1
Respirable	2700	(45)	FWS-B	343	DM-800	1	0.3
Respirable	2700	(45)	FWS-B	155	DM-800	-8	0
Respirable	960	(16)	FWS-B	91	PMM	1.2	1.3
Respirable	1500	(25)	FWS-B	89	RDM	---	0
						Mean	0.4 ± .6

[a] Aerosol MMAD = 3.4 μm; σ_g = 2.0.

[b] Respirable dust defined as material passing a 10-mm nylon cyclone operated at 2.0 ℓ/min.

1. **Effect of Charge Upon Aerodynamic Particle Size Distribution.** The size distributions of charged and neutralized coal dusts were measured in low humidity in the SIC aerosol chamber. A total of six experiments used alternately a dummy (empty) charge neutralizer and a tritium-filled holder (Sec. II) to produce charged or neutralized coal dust clouds. The particle size distribution in the clouds was measured using six-stage AI to determine whether selective deposition losses from the charged cloud would change the size distribution significantly. The results (Table VII) indicate that the charged aerosol is not significantly different. Thus, other charge effects could be measured without the complication of comparing aerosols of significantly different particle size distributions.

2. **Quantitative Charge Measurements.** The magnitude and polarity of the charge on a coal dust cloud under various conditions were measured to determine the effectiveness of the neutralization techniques. During the charge measurements, the SIC aerosol system generated a charged coal dust, part of which was withdrawn from the chamber and passed through the charge-measuring apparatus shown in Fig. 28. The apparatus included several particle charge collectors and a humidification device to precondition the supply air. Charge was measured by passing 10 ℓ/min of coal dust through the parallel-plate ion collector or 2 ℓ/min through a concentric electrode ion collector. A preweighed 47-mm-diam membrane filter downstream of the ion collector determined the amount of coal dust that penetrated the ion collector. This mass was subtracted from the chamber concentration to determine the collected mass or mass contributing the measured charge.

Initial charge measurements were made using a Wesix ion collector which consists of seven parallel plates with alternate plates connected to opposite electrical potentials. Current flow between the plates was measured to determine total charge on the aerosol. This arrangement was used to gather preliminary data on airflow, necessary collection potential, and collection efficiency. During these tests, air leaks were discovered in the ion collector so the entire ion collector was enclosed in a leakproof container. Unfortunately, this container's large outer surface made the measurement system sensitive to induced capacitance and image charge, resulting in

TABLE VII

EFFECT OF CHARGE UPON COAL AEROSOL PARTICLE SIZE DISTRIBUTION

No. of Samples	Dust	Condition	Size Parameters[a] MMAD (μm)	σ_g
11	Standard	Charged	3.5 ± 0.23 (6.6%)[b]	2.0 ± 0.12 (6%)
11	Standard	Neutralized	3.7 ± 0.25 (6.8%)	2.0 ± 0.13 (6.5%)

[a]Defined by Andersen impactor.

[b]Numbers in parentheses are coefficients of variation.

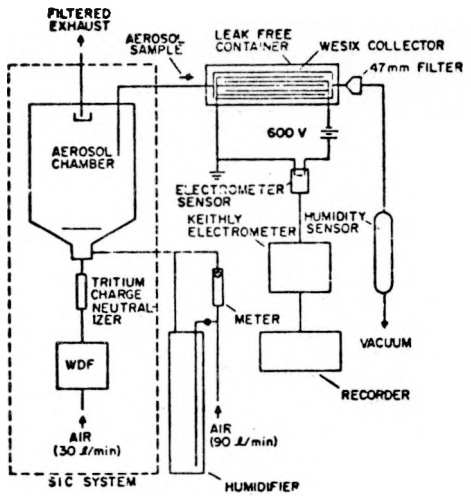

Fig. 28.
Electrical charge measurement apparatus schematic.

high noise background. A concentric charge collector with a smaller surface was then constructed. It was a 2.54-cm-diam by 25-cm-long, copper tube, outer grounded collector, with a 1-cm-diam center rod serving as the charged electrode. This collector significantly decreased electrical noise; however, a lower flow rate (~2 ℓ/min) and a higher potential (~750 V/cm) were required to collect the coal dust satisfactorily.

Current through the ion collector was measured using a Keithly vibrating capacitor electrometer that measured currents as low as 10^{-15} A. Measuring current of this magnitude required careful exclusion of spurious voltages and capacitance effects. The input resistance of the electrometer pickup head could be as high as 10^{16} ohms for very low measurements. However, usually, 10^{10} to 10^{12} ohms were sufficient. All possible leakage paths had significantly higher resistances to ensure accurate measurement of particle charge. This required short, well-insulated conductors and clean Teflon insulators between the collector electrodes. Careful attention to these points, and use of an annular collector, provided signal-to-noise ratios of >100 for most measurements.

Relative humidity in the chamber was initially regulated by bubbling part of the dilution air through water heated to ~90°C. This air was then mixed with dry dilution air to get the desired relative humidity. For high humidities (>50%), the current measured on neutralized aerosol was higher than that on dry, unneutralized aerosol. These results suggested that charged water droplets were being generated by the bubbling air. To eliminate these possible droplets, air was passed through loosely packed, water-saturated wood chips for humidification and then passed through a membrane filter before dilution of the aerosol. Despite these modifications, moist air gave high currents (Table VIII). High background currents were also noted in clean, moist air with zero potential across the ion collector. Possible causes of high background currents include increased electrical conductivity of the humid air and/or higher conductivity of resistance paths between electrodes.

The average charge on the coal aerosol generated from standard coal dust was 7.9 x 10^{-6} C/g. These data were used with the aerosol's aerodynamic particle size distribution and the collected mass data to calculate an average charge per aerodynamic equivalent particle. This charge was 180 e^-/particle. In agreement with another study[28] of coal aerosols generated from metal generators, this charge was negative. The results of charge measurements on various aerosols are given in Table VIII. The aerosol history is defined in the comments column. "Total dust"

TABLE VIII

ELECTRIC CHARGE ON COAL DUST AEROSOLS

No. of Measurements	Total Charge (c/g)	Average Charge (F⁻/Particle) Based on MMAD	Based on CMD	Relative Humidity (%)	Comments
15	7.9×10^{-6}	180 ± 40	63 ± 14	<10	Total dust, charged
14	1.0×10^{-7}	1.8 ± 1.2	0.8 ± 0.6	<10	Total dust, neutralized
4	1.3×10^{-5}	125 ± 30	-	12	Respirable, charged
4	1.8×10^{-7}	1.3 ± 1.0	-	15	Respirable, neutralized
3	1.0×10^{-5}	230 ± 20	-	63	Total dust, charged
2	8.5×10^{-5}	~1900	~677	89	Total dust, charged

designates aerosols taken directly from the chamber; "cyclone" designates measurements made on the aerosol penetrating a 10-mm nylon cyclone operated at 2 ℓ/min; "neutralized," one that passed through the tritium charge neutralizer; and "charged," one that passed through the dummy neutralizer. The measured charge on neutralized aerosols taken directly from the chamber, or after passing through the cyclone indicates that the 200-mCi neutralizer effectively removes charge under these conditions. The slight charge difference of the unneutralized aerosol after it passes through the cyclone suggests that selective collection of charged particles by the cyclone is minimal.

3. Personal Sampler Performance in Charged Coal Dust. Finally, the performance of personal samplers in charged and uncharged aerosols was compared. The SIC unit was used to generate 3.5 to >6 mg/cm³ of the standard test dust. Up to six personal samplers, including two with 10-mm-diam stainless steel cyclones instead of the normal nylon presampler, were operated in the chamber. A sampling flow rate of 2 ℓ/min for 2 h was used.

Table IX shows the results, which indicate no significant difference in separation characteristics of personal samplers operated in charged and neutralized coal dust clouds. Moreover, the standard nylon personal samplers perform essentially the same as grounded stainless steel (conductive) cyclones in these circumstances. However, the coefficients of variation suggest that the nylon cyclones may perform more erratically in charged clouds than in neutralized clouds, and more erratically than do stainless steel cyclones in either type of cloud.

E. Conclusion

Except for the study of personal air sampler loading with time, the investigations described in this section confirmed previous investigators' work. Electrical charge does not seem to affect the separation characteristics under the conditions investigated. Calibration of the personal sampler cyclone agreed with two previous reports but disagreed with another.

Only the sampler loading results departed from others' conclusions that there was no significant loading during long-term operation. Our results showed that use of a particular type of filter aggravated the low estimate of respirable dust provided by a 2-ℓ/min flow rate. During long-term operation, these two effects combined to give respirable dust estimate errors of up to 23%.

TABLE IX

EFFECT OF CHARGE ON CYCLONE PENETRATION

Aerosol Condition	Cyclone Penetration			
	Stainless Steel Cyclone		Nylon Cyclone	
	No. of Samples	%	No. of Samples	%
Charged	16	42.8 ± 2.2 (5.2)[a]	32	41.8 ± 3.4 (8.1)
Neutralized	14	42.7 ± 2.0 (4.8)	28	42.4 ± 2.2 (5.1)

[a]Numbers in parentheses indicate coefficient of variation.

ACKNOWLEDGMENT

The advice and support of George A. Carson and Larry Doemeny, the NIOSH Project Officers during this program, are gratefully acknowledged. The assistance of Bonnie Isom, Electron Microscopist, and Don Gettemy, Technician, was essential to the completion of the work.

REFERENCES

1. J. Cartwright and J. W. Skidmore, "The Size Distribution of Coal and Rock Dusts in the Electron and Optical Microscope Ranges," Ann. Occup. Hyg. **3**, 33-57 (1961).

2. J. W. J. Fay and J. R. Ashford, "Size Distribution of Airborne Dust Samples from British Coal Mines," Brit. J. Appl. Phys. **11**, 2-13 (1960).

3. H. J. Ettinger and G. W. Royer, 'Calibration of a Two-Stage Sampler," Amer. Ind. Hyg. Assoc. J. **31**, 537-545 (1970).

4. M. Lippmann and W. B. Harris, "Size-Selective Samplers for Estimating Respirable Dust Concentrations," Health Phys. **8**, 155 (1962).

5. R. H. Knuth, "Recalibration of Size-Selective Samplers," Amer. Ind. Hyg. Assoc. J. **30**, No. 4, 379 (1969).

6. "Threshold Limit Values for Chemical Substances and Physical Agents in the Workroom Environment with Intended Changes for 1975," Amer. Conf. of Gov't Ind. Hyg. (1975).

7. B. M. Wright, "A New Dust-Feed Mechanism," J. Sci. Instr. **27**, 12-15 (1950).

8. P. Lilienfeld and J. Dulchinos, "Portable Instantaneous Mass Monitor for Coal Mine Dust," Amer. Ind. Hyg. Assoc. J. **33**, 136-145 (1972).

9. H. J. Ettinger and S. Posner, "Evaluation of Particle Sizing and Aerosol Sampling Techniques," Amer. Ind. Hyg. Assoc. J. **26**, 17-25 (1965).

10. J. G. Olin, G. J. Sem, and D. L. Christenson, "Piezoelectric-Electrostatic Aerosol Mass Concentration Monitor," Amer. Ind. Hyg. Assoc. J. **32**, 209-220 (1971).

11. B. P. Almich and G. A. Carson, "Some Effects of Charging on 10-mm Nylon Cyclone Performance," Amer. Ind. Hyg. Assoc. J. **35**, 603-612 (1974).

12. M. Roder, National Institute for Occupational Safety and Health, personal communication, July 1973.

13 B. Almich, National Institute for Occupational Safety and Health, personal communication, September 1974.

14. O. R. Moss and H. J. Ettinger, "Respirable Dust Characteristics of Polydisperse Aerosols," Amer. Ind. Hyg. Assoc. J. **31**, 546-547 (1970).

15. J. R. Lynch, "Evaluation of Size-Select Cyclone and Elutriator Relationships," Amer. Ind. Hyg. Assoc. J. **31**, 548-551 (1970).

16. S. Brunauer, P. H. Emmett, and E. Teller, "The Adsorption of Gases in Multimolecular Layers," J. Am. Chem. Soc. **60**, 309 (1938).

17. P. C. Carman and P. le R. Malherbe, "Routine Measurement of Surface of Paint Pigments and Other Fine Powders," J. Soc. Chem. Ind. **69**, 134-143 (1950).

18. J. C. Arnell and P. C. Carman, "Surface Area Measurements of Fine Powders Using Modified Permeability Equation," Can. J. Research, **26A**, 128-136 (1948).

19. N. Thaulow and E. W. White, "General Method for Dispersion and Disaggregation of Particulate Samples for Quantitative SEM and Optical Microscope Studies," Powder Tech. **5**, (6), 377-379 (1971).

20. L. W. Ortiz and B. L. Isom, "Transfer Technique for Electron Microscopy of Membrane Filter Samples," Amer. Ind. Hyg. Assoc. J. **35** (7), 423-425 (1974).

21. A. A. Andersen, "A Sampler for Respiratory Health Hazard Assessment," Amer. Ind. Hyg. Assoc. J. **27**, 160-165 (1966).

22. Andersen 2000, Incorporated Technical Sales Brochure, pg. 10, Andersen 2000 Incorporated, Atlanta, Georgia (1972).

23. P. Kotrappa and M. E. Light, "Design and Performance of the Lovelace Aerosol Particle Separator," Rev. Sci. Instrum. **43** (8), 1106-1112 (1972).

24. T. Hatch and S. P. Choate, "Statistical Description of the Size Properties of Non-Uniform Particulate Substances," J. Franklin Inst. **207**, 369-387 (March 1929).

25. P. Kotrappa, "Shape Factors for Aerosols of Coal, UO_2, and ThO_2 in the Respirable Size Range," Chap. 16, **Assessment of Airborne Particles**, T. T. Mercer, P. E. Morrow, and W. Stober, Eds. (Charles C. Thomas, Springfield, Illinois, 1972).

26. K. J. Caplan, L. J. Doemeny, and S. Sorenson, "Evaluation of Coal Mine Dust Personal Sampler Performance," (final report) NIOSH Contract CPE-R-70-0036 (November 1973).

27. T. F. Tomb and L. D. Raymond, "Evaluation of the Penetration Characteristics of a Horizontal Plate Elutriator and of a 10-mm Nylon Cyclone Elutriator," U. S. Bureau of Mines report RI 7376 (March 1970).

28. W. Schnabel, "The Charging and Adhesion of Small Particles," Staub (Eng) **28** (11), 19-24 (1968).

APPENDIX

ELECTRIC CHARGE ON COAL AEROSOL

The measured charge on coal aerosols generated from the WDF and the size distribution of the standard coal dust can be used to calculate the amount of tritium required to neutralize the charge.

Given the maximum design conditions of 30-ℓ/min flow through the WDF plus 90 ℓ/min of dilution air, and 6-μg/ℓ dust concentration in the chamber, the aerosol concentration leaving the WDF is 24 μg/ℓ (2.4×10^{-5}g/l). Converting this mass concentration to generator mass output gives 1.2×10^{-5}g/s leaving the WDF (and passing through the neutralizer).

From Table VIII (Sec. IV), the total charge is 7.9×10^{-6}C/g or 4.93×10^{13}|e|/g and the charge generated every second is, therefore, 5.9×10^{8} |e|/s.

Considering the ionization available for neutralizing charge on the particles, the average energy of the tritium β-decay is 5×10^{3} eV and 32 eV is required to form an ion pair in air. Assuming that 50% of the β^- decays are toward the metal, the number of ion pairs produced per second for each curie of tritium is given by

$$1.65 \times 10^{10} \ \frac{\text{dis.}}{\text{sec-Curie}} \times 5 \times 10^{3} \text{ ev} \times \frac{1}{32} \ \frac{\text{ion pair}}{\text{ev}} = 2.58 \times 10^{12} \ \frac{\text{ion pair}}{\text{Curie-sec}} \ .$$

These ion pairs are formed in a dense path, so recombination will be quite high. Assuming conservatively that 99.9% of the ion pairs recombine, 2.58×10^{9} ion pairs/s-Ci will be available to discharge the aerosol.

Finally, the required amount of tritium is given by

$$\frac{5.9 \times 10^{8} |e|/\text{sec}}{2.58 \times 10^{9} |e|/\text{sec-Curie}} = 2.28 \times 10^{-1} \text{ Curies} \ ,$$

or, a maximum of 228 mCi is required to neutralize the aerosol charge.

The experimental arrangement shown in Fig. A-1 determined the approximate amount of tritium needed to eliminate charge on the coal aerosol. Ion collector voltage was held constant at 1500 V (E = 1500 V/cm), and the current was measured as the amount of tritium was decreased

by covering the tritide foil with thin cardboard. The current did not increase until more than 96% of the tritide had been covered. The current measured when 3.1% of the tritium was available was 25% of that measured when none was available. (The zero tritium level was determined using an empty tritide holder.) The current readings were the same for all measurements made with more than 3.1% of the tritium available, and amounted to 8% of the current measured with the tritium foil removed. This indicates that if >125 mCi (3.1% of the 4-Ci tritium source) is available, the test aerosol is adequately discharged.

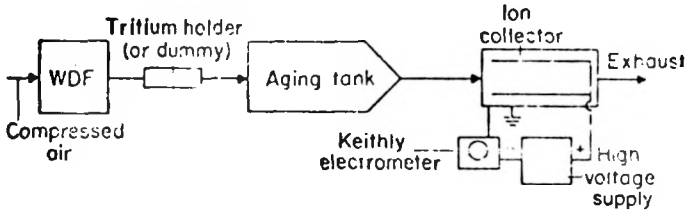

Fig. A-1.
Aerosol charge measurement apparatus.